Powder Technology (2009)
DOI: http://dx.doi.org/10.1016/j.powtec.2009.07.022
Accepted Postprint

Hydrodynamics of regular particles in a liquid-solid semi-fluidized bed

H. M. Jena[1*], G. K. Roy[1] and B. C. Meikap[2]

[1]*Department of Chemical Engineering, National Institute of Technology (NIT), Rourkela, Orissa, Pin - 769008, India*

[2]*School of Chemical Engineering, Howard College, University of Kwazulu-Natal, Durban-4041, South Africa*

* Corresponding Author. Tel.: +91-661-2462264;
Fax: +91-661-2462999
E-mail address: hara.jena@gmail.com

Abstract

Semi-fluidized bed hydrodynamics, including minimum and maximum semi-fluidization velocities, packed bed formation and pressure drop across the bed, have been studied in a 0.1 m ID liquid-solid semi-fluidized bed. The top grid is a specially designed perforated plate to have negligible pressure drop across it and to retain all the particles used in the experiment. Experimental parameters studied included velocity, density and viscosity of the liquid, particle size, static bed height and expansion ratio. Empirical and semi-empirical models have been derived. The results have been compared with those available in the literature.

Keywords: Hydrodynamics; Liquid-solid semi-fluidization; Pressure drop; packed bed height; minimum and maximum semi-fluidization velocity; viscosity effect.

1. Introduction

A semi-fluidized bed can be viewed as the combination of a batch fluidized bed at the bottom and a fixed bed at the top within a single vessel. Such a bed can be formed by providing sufficient space for the free expansion of a fluidized bed and then arresting the escape of particles by means of a top restraint. The degree of semi-fluidization occurring in the bed can range from minimum semi-fluidization (the expanded fluidized bed first touches the top restraint of the semi-fluidizer) to maximum semi-fluidization (where all the solid particles attach to the top restraint) by varying the liquid velocity or by altering

the position of the upper constraining plate. A semi-fluidized bed has the advantages of both the packed and the fluidized beds. The disadvantages of fluidized beds, namely back-mixing of solids, attrition of particles and erosion of surfaces, and those of packed beds, such as non-uniform bed temperatures, segregation of solids and channeling, are taken care of, at least partially in a semi-fluidized bed [1, 2].

The development and advantages of the semi-fluidized bed relating to studies on hydrodynamics, mass transfer, reaction kinetics and filtration have been highlighted by Murthy and Roy [1] and Ho et al. [2]. Subsequently a good number of research articles relating to various applications of the semi-fluidized bed system have been reported in literature [3-14]. Additionally, fairly a good number of patents claimed since the year 1958, relating to the best possible applications of the semi-fluidized bed in many industrial processes are listed in SciFinder Scholar database like the recent one by Liu et al. [15]. In these investigations, either in gas-solid or liquid-solid systems, particle sizes varying from very small size to very large size (0.04 m) have been employed as the bed material. Kurian and Raja Rao [16] have studied hydrodynamic behaviour of particles in the size range of 0.000548 to 0.00467 m, but except the 0.00467 m particle all others are highly irregular in shape (sphericity in the range 0.68 to 0.76). However they have not studied the viscosity effect. Fan and Hsu [17] have discussed the suitability of the semi-fluidized bed as a bioreactor for aerobic and anaerobic applications. Later Dias [3] has mentioned the significant performance of the semi-fluidized bed system in the extractive fermentation of ethanol. In the immobilized cell bioreactors the preferred size of the solid matrix is nearly 2 - 4 mm. The information available on the hydrodynamics of moderately large size particles in a semi-fluidized bed is also limited.

In the present study the experimental system used ultimately aims at the use of a semi-fluidized bed as an aerobic as well as an anaerobic bioreactor. The objective of this work is to investigate the hydrodynamics of semi-fluidization in liquid-solid systems, including the minimum and the maximum semi-fluidization velocities, the packed bed formation and the pressure drop across the bed. Experiments have been carried out in a 0.1 m ID column. Glass beads of four different sizes were used as the solid phase. Aqueous solutions of glycerol have been used as the liquid phase. The effect of the system parameters studied is superficial liquid velocity, liquid density, liquid viscosity, particle size, static bed height and bed expansion ratio. The observed results have been correlated with the system variables and compared with the data available in the literature.

2. Experimental Set-up and Technique

A schematic representation of the experimental setup is shown in Fig. 1. The experimental semi-fluidized bed consists of a fluidized bed assembly, a top restraining plate with fixture, and a pressure measuring arrangement. The fluidized bed assembly consists of a fluidizer, liquid distributor, liquid disengagement and recirculation facility, liquid pump, liquid storage tank, a set of calibrated liquid rotameters.

The fluidizer is a vertical cylindrical Plexiglas column of 0.1 m internal diameter and 1.25 m height. The liquid distributor is located at the bottom of the fluidized bed column and is designed in such a manner that uniformly distributed liquid enters the fluidized bed column. The distributor section made of Perspex is fructo-conical of 0.31 m in height, and has a divergence angle of 4.5^0 with the bottom end of 0.0508 m and the top

end of 0.1 m in internal diameter respectively. The liquid inlet of 0.0254 m in internal diameter is located centrally at the lower cross-sectional end. The higher cross-section end is fitted to the fluidized bed column, with a perforated distributor plate made of G.I. sheet of 0.001 m thick, 0.12 m diameter having open area equal to 20 % of the column cross-sectional area with a 16 mesh (BSS) stainless steel screen in between. Totally 288 number of 0.002 m, 0.0025 m and 0.003 m holes have been drilled in triangular pitch made in 10 concentric circles of nearly 0.005 m radial gap. The size of the holes has been increased from inner to outer circle. This has been done with a view to have less pressure drop at the distributor plate and a uniform flow of the liquid into the test section. The liquid disengagement section at the top of the column is a cylindrical section of 0.026 m internal diameter and 0.034 m height, assembled to the fluidized bed column with 0.08 m of the fluidized bed column inside it, which allows little hold up of the liquid and liquid to be circulated through the outlet of 0.0254 m internal diameter at the bottom of this section.

The top restraining plate is made from Perspex sheet of 0.099m diameter and 3 mm thick containing 3, 4 and 5 mm holes with approximate total open area of 40%. There is a minor clearance between the plate and the inner wall of the column, which facilitated the free movement of the plate in the column, restricting the particle entrainment. A BSS 16 mesh screen is attached to the bottom of the plate and the plate is supported by a Perspex slotted support from the top. The whole assembly is fitted to an iron rod of 8 mm diameter with nut bolt arrangement. The photographic view of the top restraint is presented in Fig. 1.

For pressure drop measurement in the bed, the pressure taps of 6 mm diameter have been connected to the manometers filled with carbon tetrachloride and mercury. Pressure taps have been installed vertically along the bed at a distance of 0.1 m between each pressure tap. The inside opening of each tap is screened to prevent penetration of the bed particles.

Glass beads of four different sizes and aqueous solutions of glycerol have been used as the solid and the liquid phases respectively. The scope of the experiment is presented in Table 1. Accurately weighed amount of material is fed into the column, fluidized and de-fluidized slowly and adjusted for a specified reproducible initial static bed height. Liquid is pumped to the fluidizer at a desired flow rate using liquid rotameter. Three calibrated rotameters with different ranges have been used for the accurate record of the flow rates. Approximately five minutes are allowed to make sure that the steady state has been reached. The readings of the manometers and the expanded bed heights or the top packed bed height (as the case may be) are then noted. The procedure has been repeated varying the particle size, viscosity and density of the liquid, bed expansion ratio (R) and initial static bed height.

3. Results and Discussion

Experiments have been conducted with the superficial liquid velocity varying from 0 to 0.3057 m/s. The temperature is maintained at 30 ± 2^0C. To ensure steady state in operation at least five minutes have been allowed before each reading. Readings for expanded bed height, pressure drop and top packed height have been noted down. The experimental results have been presented graphically in this section. Empirical and semi-empirical equations have been developed.

3.1 Minimum semi-fluidization velocity

The minimum semi-fluidization velocity also called the onset velocity of semi-fluidization (U_{osf}) is the superficial liquid velocity at which a bed particle of the expanded fluidized bed first touches the top restraint of the semi-fluidizer. Experimentally the minimum semi-fluidization velocity can be determined by the following methods. (1) From the plot of the ratio of the height of the top restraint to the height of the expanded fluidized bed (H_t/H_f) versus the superficial liquid velocity (U_l) as illustrated in Fig. 2. (2) From the plot of pressure drop across the bed versus the superficial liquid velocity as illustrated in Fig. 3. (3) For comparatively large particles from the visual observation. As the top portion of the fluidized bed is dilute in particles it is practically difficult to mention the exact height of the expanded bed. In such a case if the height of the expanded bed is taken as the height of the moderately dense bed then it predicts higher value of U_{osf}. Otherwise if the top surface of the dilute bed is taken the method predicts lower value of U_{osf}. The pressure drop method seems to be the best one. Ho et al. [2], Fan and Wen [18], Roy and Sarma [19], and Roy and Sharat Chandra [20] have recommended the pressure drop method for the prediction of U_{osf}.

In the present work the values of the minimum semi-fluidization velocities have been experimentally obtained by both the methods (1) and (2) and reported in Table 2, but the values from method-2 have been used for the development of the model equations. In the present investigation the minimum semi-fluidization velocity obtained from method-1 have been found to be higher than those obtained from method-2. Fig. 4 shows the almost negligible effect of initial static bed height on the minimum semi-fluidization velocity. The independency of U_{osf} on static bed height for the liquid-solid

system has been reported by Roy and Sarma [19] and Roy and Sharat Chandra [20]. But Ho et al. [2] have reported that the static bed height slightly affects the minimum semi-fluidization velocity in a gas-solid semi-fluidized bed. They have reported a decrease in the minimum semi-fluidization velocity with the increase in initial static bed height. This may be true as the reasoning given by them is that an increase in static bed height corresponds to an increase in bubble size, which in turn promotes the bed expansion and accelerates the semi-fluidization process. But the phenomenon is not observed in case of a liquid-solid system, thus the minimum semi-fluidization velocity being practically un-affected by the initial static bed height.

The effect of particle size on U_{osf} is presented in Fig. 5. This shows that larger the particle size higher is the minimum semi-fluidization velocity. This is true as higher drag force and ultimately the higher fluid velocity is required to lift the bigger size particle which bears a higher mass. The bed expansion ratio has a strong effect on the minimum semi-fluidization velocity as indicated in Fig. 6. The reason is the requirement of higher fluid velocity to lift the particle to a relatively higher position of the top restraint in the bed. U_{osf} increases with the increase in bed expansion ratio. The same behaviour has been observed by other investigators also.

To study the effect of liquid viscosity, aqueous solutions of glycerol (0 – 24 % by mass) have been used as the liquid phase. The properties of the solutions are given in Table 1. For the glycerol solutions there is an increase both in the density and viscosity with increase in percentage of glycerol in the solution. The increase in viscosity is predominant over density as increase in viscosity is 96.7% for 24% glycerol solution over the water; where as the increase in density is only 5.85% for the same solution. Thus the

study on viscosity effect using these solutions is not far away from the assumption of the constant density. The effect of liquid viscosity on the minimum semi-fluidization velocity is shown in Fig. 7. The figure indicates the decrease in the minimum semi-fluidization velocity with increase in the liquid viscosity. This is due to the fact that the particles achieve higher drag at lower velocity of the liquid possessing higher viscosity.

Kurian and Raja Rao [16] have suggested two theoretical methods for the estimation of U_{osf}. The first method is based on the correlation for the expanded bed voidage.. Use of this method is not convenient as one has to use the proposed expanded bed voidage correlation along with the correlation graph given in their published article [16]. The second method is based on the correlation for the height of the top packed section (h_{pa}), which is discussed in detail in the following section *3.4*. At the onset of semi-fluidization, h_{pa}=0, the correlation is given by

$$\frac{U_{osf} - U_{mf}}{U_t - U_{mf}} = 0.61\left(\frac{R}{R-1}\right)^{-1.2} \qquad [1]$$

In the present work, the observed minimum semi-fluidization velocity has been correlated with the static bed height, bed expansion ratio, particle size and liquid viscosity. The following equation with a correlation coefficient of 0.977 has been obtained.

$$U_{osf} = 0.14R^{0.9}d_p^{0.5}\mu_l^{-0.25} \qquad [2]$$

It is indicated that the minimum semi-fluidization velocity is independent of static bed height. A few more experimental runs have been carried out with glass bead of size 0.00155 m, bed expansion ratios of 1.5, 1.75, 2.25, 2.75, 3.25, 3.75 and 4.0 and liquid viscosity of 0.001752 Pa.s (30% by mass of glycerol solution) to test the validity of the

correlation in the near by range. Values of U_{osf} predicted from Eqs. (1) and (2) and the experimental ones have been reported in Table 2 and compared in Fig. 8. The Eq. (2) adequately describes the observed data with a standard deviation value of 0.0235 as indicated in Fig. 8. Values of U_{osf} predicted from Eq. (1) also shows good agreement except four points deviating more than 10%. In the figure the legend indicating the other data points means those are not used for the development of the empirical model.

3.2 Maximum semi-fluidization velocity

The maximum semi-fluidization velocity (U_{msf}) is the fluid velocity at which the entire bed of solid particles is transferred to the top packed bed. Theoretically this velocity corresponds to the terminal (free fall) velocity (U_t) of the particles. The intermediate law for gravity settling (intermediate flow) or the Newton's law (turbulent flow) as given by Gupta and Sathiyamoorthy [21] is valid for most experimental conditions and has been used for the calculation of terminal velocity.

For intermediate flow:

$$\mathrm{Re}_t = 0.153 Ar^{0.7} \qquad [3]$$

Turbulent flow:

$$\mathrm{Re}_t = 1.74 Ar^{0.5} \qquad [4]$$

Fan and Wen [18] and Kurian and Raja Rao [16] have shown some sort of suitability of these laws for their experimental conditions. But many other investigators have suggested the use of experimental determination of the maximum semi-fluidization velocity. The reason may be the following. The terminal velocity predicted from the intermediate law or Newton's law is actually valid for a single particle. These laws sometimes mislead if used as the value of the maximum semi-fluidization velocity due to

definite influence of the presence of the other particles, as well as the effect of column wall and supports. There is a definite effect of the position of the top restraining plate relative to the static bed height on U_{msf}, but the terminal velocity for a specific particle system is independent of the grid position. The terminal velocity may be used to represent U_{msf} when the position of the top grid is at a much higher level (say at infinite position). Thus it is meaningful to find the maximum semi-fluidization velocity from the experiment if possible.

In actual experiment very often it is not possible to transfer the entire particles to the top packed bed. There are two methods used for the prediction of the maximum semi-fluidization velocity from extrapolation of the experimental data. (i) By extrapolation of the porosity of the fluidized section (ε_f) vs. superficial liquid velocity curve to ε_f =1 or (ii) by extrapolation h_{pa}/h_s vs. superficial liquid velocity curve to h_{pa}/h_s =1. The extrapolation of ε_f produce quite higher values of maximum semi-fluidization velocity for the liquid-solid system. Fan and Wen [18], Kurian and Raja Rao [16] and Roy [22] have suggested the use of the second method i.e. the extrapolation h_{pa}/h_s vs. superficial liquid velocity curve to h_{pa}/h_s =1 over the former. In the present study, the second method has been used to determine the maximum semi-fluidization velocity.

The maximum semi-fluidization velocity has been found to increase with the static bed height, the particle size and the bed expansion ratio, but to decrease with the increase in the liquid viscosity as indicated in Figs. (9) - (12). Roy [22] has shown the independency of U_{msf} on static bed height and bed expansion ratio, but in the present work a significant effect of these variables has been observed. The discrepancy may be

due to the difference in geometry and design of the components of the semi-fluidized bed, particle size and shape of the particles.

The experimental values of U_{msf} have been reported in Table 2. This table also gives the values of U_{msf} calculated from the equation proposed by Roy [22] and the terminal velocity calculated from Eq. (3) or (4) for the given experimental conditions. As seen from Fig. 13, the values of the experimentally found U_{msf} are to some extent in close agreement with those predicted from Eq. (3) or (4), but deviates a lot from the prediction using the correlation of Roy [22]. Like Eq. (2), a correlation for U_{msf} has been developed as given by Eq. (5) below with a correlation coefficient of 0.972.

$$U_{msf} = 0.5 h_s^{0.35} R^{0.67} d_p^{0.62} \mu_l^{-0.47} \quad [5]$$

The equation adequately describes the observed data with a standard deviation of 0.0274 as indicated in Fig. 13.

3.3 Dimensionless minimum semi-fluidization velocity

The onset of fluidization and semi-fluidization are two consecutive events in the sequence of the operation of the semi-fluidization phenomenon. Thus many investigators have found it convenient to represent the correlation for minimum semi-fluidization velocity in the dimensionless form as ratio of the minimum semi-fluidization velocity to the minimum fluidization velocity i.e. U_{osf}/U_{mf}. A few of them have represented the dimensionless minimum semi-fluidization velocity as the function of system and operating variables directly viz. Ho et al. [2], but some other researchers (Roy and Sarma [19], Roy and Sharat Chandra [20]) have used the system and operating variables in dimensionless form. In the present work empirical equations for U_{osf}/U_{mf} have been

represented in both the forms for the convenient use of the designers. There are many correlations available for the prediction of the minimum fluidization velocity from the knowledge of the fluid and solid properties. In the present communication, the minimum fluidization velocity has been predicted from the correlation of Wen and Yu [23], used widely.

$$\mathrm{Re}_{mf} = \sqrt{33.7^2 + 0.0408Ar} - 33.7 \qquad [6]$$

The experimental values of the dimensionless minimum semi-fluidization velocity have been reported in Table 3. The dimensionless minimum semi-fluidization velocity is independent of the static bed height. For all other variables at constant value, the smaller the particle size the higher is the dimensionless minimum semi-fluidization velocity. The dimensionless minimum semi-fluidization velocity increases with the increase in bed expansion ratio. There is a slight increase in the dimensionless minimum semi-fluidization velocity (U_{osf}/U_{mf}) with the increase in liquid viscosity. In terms of system and operating variables and the variables in their dimensionless term, the dimensionless minimum semi-fluidization velocity (U_{osf}/U_{mf}) can be represented as;

$$\frac{U_{osf}}{U_{mf}} = f(h_s, D_c, d_p, \rho_s, \rho_L, \mu_l, R) \qquad [7]$$

$$\frac{U_{osf}}{U_{mf}} = f\left[\frac{h_s}{D_c}, \frac{d_p}{D_c}, \frac{\rho_s}{\rho_L}, \frac{\mu_l}{\mu_w}, R\right] \qquad [8]$$

Since the column diameter and the density of solid are constant, the variation in the liquid density is negligible and the effect of static bed height is not relevant, with the help of the remaining experimental parameters, the equations developed are;

$$\frac{U_{osf}}{U_{mf}} = 0.388 d_p^{-0.37} \mu_l^{0.1} R^{0.92} \qquad [9]$$

$$\frac{U_{osf}}{U_{mf}} = 0.45\left(\frac{d_p}{D_c}\right)^{-0.37}\left(\frac{\mu_l}{\mu_w}\right)^{1.14}(R)^{0.92} \quad [10]$$

Both the equations possess a correlation coefficient of 0.9804 and predict the same value of the dimensionless minimum semi-fluidization velocity, but appear in different forms. The values of the dimensionless minimum semi-fluidization velocity predicted from Eqs. (9) and (10) are in very close agreement with the experimental values with a standard deviation of 2.59%.

The values of the dimensionless minimum semi-fluidization velocity also calculated from the correlation available in the literature pertaining to the liquid-solid system (Roy and Sarma [19]) have been indicated in Table 3. The values predicted are much higher than the present findings. This may be due to delayed semi-fluidization in their system with difference in particle size, bed geometry of the bed and the design of the top grid which one is a fructo-conical perforated one attached to a wire mesh. But a similar dependency on the system variables has been observed in both the cases. The main contribution might be that of the particle size and the pressure gradient at the top grid. As the particle size becomes smaller the dimensionless minimum semi-fluidization velocity increases. The correlation by Roy and Sarma [19] has been developed for very small particles, thus predicting higher values of the dimensionless minimum semi-fluidization velocity.

Roy and Sharat Chandra [20] and Roy [22] have proposed a different correlation for predicting the minimum semi-fluidization velocity in the dimensionless form. The different dimensionless minimum semi-fluidization velocity (U_{osf}/U_{msf}) is the ratio of the minimum semi-fluidization velocity to the maximum semi-fluidization velocity. For the

prediction of the maximum semi-fluidization velocity they have proposed an empirical equation from their experimental findings. In this communication the dimensionless minimum semi-fluidization velocities (U_{osf}/U_{msf}) calculated from the experimental findings of minimum and maximum semi-fluidization velocities and predicted from the proposed correlation by Roy [22] has been reported in Table 3. The equation proposed by Roy [22] predicts a higher value of U_{osf}/U_{msf}. This is due to the higher values of the minimum semi-fluidization velocity as pointed earlier and lower value of maximum semi-fluidization velocity. A new correlation (Eq. (11)) has been proposed here for the prediction of U_{osf}/U_{msf}.

$$\frac{U_{osf}}{U_{msf}} = 0.254\left(\frac{h_s}{D_c}\right)^{-0.3}\left(\frac{d_p}{D_c}\right)^{-0.05}\left(\frac{\mu_l}{\mu_w}\right)^{0.16}(R)^{0.3} \qquad [11]$$

Like the dimensionless minimum semi-fluidization velocity, the maximum semi-fluidization velocity can also be represented in dimensionless form as dimensionless maximum semi-fluidization velocity (U_{msf}/U_{mf} or U_{msf}/U_{osf}). U_{msf}/U_{osf} is the inverse of U_{osf}/U_{msf} and can be predicted from Eq. (11) just by inversion. Earlier Roy and Sarma [24] have proposed one correlation for U_{msf}/U_{mf} for the liquid-solid system with irregular particles, where only the effect of two variables i.e. the particle size and the particle density is shown. In the present work a new correlation (Eq. (12)) has been developed from experimental values of U_{msf}/U_{mf} with a correlation factor of 0.973. The values of U_{msf}/U_{mf} predicted from the correlation of Roy and Sarma [24] have been indicated in Table 3 along with the experimental values. Most of the values are within +20 % except those corresponding to the bed expansion ratio, R = 2 and for values withviscosity

variation. The difference may be due to the absence of variable like: liquid viscosity, expansion ratio and static bed height in the correlation of Roy and Sarma [24].

$$\frac{U_{msf}}{U_{mf}} = 1.565\left(\frac{h_s}{D_c}\right)^{0.36}\left(\frac{d_p}{D_c}\right)^{-0.33}\left(\frac{\mu_l}{\mu_w}\right)^{-0.08}(R)^{0.69} \qquad [12]$$

3.4 Packed bed formation

Between the two limiting conditions of semi-fluidization i.e. the minimum and the maximum, a part of the total solid form a packed bed beneath the top restraint plate, while the balance of the solid remain in the fluidized state. By adjusting the position of the top grid and / or by varying the velocity of the fluid, the extent of packed bed formation can be controlled to suit to a particular requirement. The extent of packed bed formation is also closely related to the pressure drop across the semi-fluidized bed. The prediction of packed bed formation is therefore important in the study of semi-fluidization.

In the present study the packed bed formation has been represented as dimensionless quantity such as h_{pa}/h_s and $(h- h_{pa})/(h- h_s)$. The voidage of the top packed bed has been assumed to be equal to the voidage of the reproducible initial static bed. The dependency of h_{pa}/h_s on superficial liquid velocity, bed expansion ratio, static bed height, particle size and liquid viscosity are shown in Fig. (9) through (12). The results indicate that the packed bed section starts to form at a velocity right above the minimum semi-fluidization velocity, and the section increases in height as the velocity is increased. The packed bed height increases with the liquid velocity, but decreases with bed expansion ratio, particle size and to a lesser extent on the initial static bed height. As mentioned by Ho et al. [2], in the present study the formation of packed bed for the liquid-solid system

has not been uniform. The mean packed bed height from the repeat of the experiments has been taken as the packed bed height under each operating condition.

Fan and Wen [18], using dimensional analysis and the momentum and continuity equations, obtained the following relationship.

$$[(h- h_{pa})/(h- h_s), (U_s- U_{mf})/(U_{msf} -U_{mf})] = 0. \quad [13]$$

Using this relation Kurian and Rao [16], proposed the following correlation from their experimental finding.

$$\frac{U_s - U_{mf}}{U_t - U_{mf}} = 0.61\left(\frac{h - h_{pa}}{h - h_s}\right)^{-1.2} \quad [14]$$

Singh et al. [25], have proposed a different correlation in the logarithmic form from their experimental finding as indicated below.

$$\frac{h - h_s}{h - h_{pa}} = 0.974 + 0.324\ln\left(\frac{U_s - U_{mf}}{U_t - U_{mf}}\right) \quad [15]$$

Mydlarz [26], from his experimental finding has shown the validity of Eq. (14) for the range of the dimensionless packed bed height as; $1.3 < (h- h_{pa})/(h- h_s) < R$. He has proposed a different relation for the range $1.0 < (h- h_{pa})/(h- h_s) < 1.3$ as;

$$\frac{U_s - U_{mf}}{U_t - U_{mf}} = \left(\frac{h - h_{pa}}{h - h_s}\right)^{-3.15} \quad [16]$$

In the present study an attempt has been made to correlate the experimental data for the larger regular particles in the form of the Eqs. (14) – (16). The following relationships have been obtained valid for the entire range of experimentation.

$$\frac{h - h_s}{h - h_{pa}} = 1.104\left(\frac{U_s - U_{mf}}{U_t - U_{mf}}\right)^{0.48} \quad [17]$$

and

$$\frac{h-h_s}{h-h_{pa}} = 1.04 + 0.3514 \ln\left(\frac{U_s - U_{mf}}{U_t - U_{mf}}\right) \quad [18]$$

The values of $(h- h_s)/(h- h_{pa})$ predicted from the Eqs. (17) and (18) have been compared with the experimental values and a fairly good agreement has been found with standard deviation values of 7.62 % and 7.46 % respectively. Fig. 14 shows the comparison of the values of $(h- h_s)/(h- h_{pa})$ predicted from Eqs. (14) – (17) with the experimental ones. Almost all values are within 15 % of the experimental ones in case of these equations. The recommendation for the use of two different power law correlation for the two different range of the values of $(h- h_{pa})/(h- h_s)$ by Mydlarz [26] is found to be true as it is seen from Fig. 14.

An attempt has been made to develop dimensionless correlation for h_{pa}/h_s in terms of dimensionless parameters U_s/U_{osf}, h_s/D_c, d_p/D_c, R and μ_l/μ_w to realize the direct effect of these variables on the packed bed height. It has been observed that upto 42% of the particles in the top packed bed i.e. $h_{pa}/h_s = 0.42$, the dependency of h_{pa}/h_s on U_s/U_{osf} is different from that of $h_{pa}/h_s > 0.42$. Thus two different correlations have been proposed to predict the packed bed formation for the different range of the values of h_{pa}/h_sas Eqs. (19) and (20). Over the specified range the predicted values of h_{pa}/h_s from Eq. (19) agrees with the experimental ones with a standard deviation value of 16.7%, where as the values predicted from Eq. (20) agrees with a standard deviation value of 9.45% as indicated in Fig. 15. This indicates the instability in the packed bed formation upto nearly 42% of the particles forming the top packed bed.

$$\frac{h_{pa}}{h_s} = 0.05\left(\frac{U_s}{U_{osf}}\right)^{6.6}\left(\frac{h_s}{D_c}\right)^{-0.08}\left(\frac{d_p}{D_c}\right)^{-0.21}\left(\frac{\mu_l}{\mu_w}\right)^{0.09}(R)^{-0.42} \quad [19]$$

for $h_{pa}/h_s < 0.42$.

$$\frac{h_{pa}}{h_s} = 0.325\left(\frac{U_s}{U_{osf}}\right)^{0.97}\left(\frac{h_s}{D_c}\right)^{-0.05}\left(\frac{d_p}{D_c}\right)^{-0.13}\left(\frac{\mu_l}{\mu_w}\right)^{0.05}(R)^{-0.26} \quad [20]$$

for $h_{pa}/h_s > 0.42$.

Fig. 16 shows the formation of and breakage behaviour of the top packed bed with increase and decrease in the liquid velocity respectively of 0.00218 m particles with R=2.0. A hysteresis loop results with significant gap between the formation and breakage of the packed bed. As seen from the plot the liquid velocity increased from 0 to 0.1911 m/s and then decreased to 0 m/s. At 0.1911 m/s liquid velocity h_{pa}/h_s = 0.885. With decrease in liquid velocity from this value, the amount of particles in the top packed bed remain intact, the expanded fluidized bed height decreases and the clear zone (portion of the bed without solid, i.e. between fluidized bed and top packed bed or top grid) in the bed increases as seen in Fig. 17. At the liquid velocity of 0.0573 m/s, particle from top packed bed starts to fall, the clear zone in the bed decreases and in a very narrow range of liquid velocity (0.0573-0.04 m/s) all the particles from the top packed bed falls to the fluidized bed at the bottom. With further decrease in the liquid velocity, the clear zone increases up to the liquid velocity reaching the minimum fluidization velocity, where the expanded bed height becomes equal to the reproducible static bed height. Thus a valley for clear zone is created between the liquid velocities corresponding to the starting of packed bed breakage and the minimum fluidization velocity as seen in Fig. 17.

3.5 Pressure drop across the bed

The pressure drop across a semi-fluidized bed can be viewed as the combination of the pressure drop across the fluidized section, the packed section and the constraint (top restraining) plate.

$$\Delta P_{sf} = \Delta P_f + \Delta P_{pa} + \Delta P_r \quad [21]$$

Ho et al. [2], Fan and Wen [18], and Kurian and Raja Rao [16] have proposed models for the prediction of bed pressure based on the above assumption. Fan and Wen [17] have neglected the pressure drop across the top restraint plate where as, Ho et al. [2] in their work with gas-solid system and Kurian and Raja Rao [16] for liquid-solid system have shown significant contribution of the pressure drop across the top restraint plate towards the total pressure drop across the semi-fluidized bed. In these models for the fluidized bed pressure drop, they have considered the amount of solids in the fluidized section of the semi-fluidized bed, but actually when the operation starts from the initial static bed, first all the solids come to the fluidization regime and then form the packed bed beneath the top grid with increase in the liquid velocity. Thus the pressure drop for the total solids of the bed for fluidization should be taken into account. This pressure drop actually gets added to the packed bed pressure drop and the pressure drop for the top restraining plate.

In the present study we have taken the pressure equivalent to the buoyant weight of whole of the solids as the fluidized bed pressure drop. The mass of the solids used in each experiment have accurately been measured and have been used for the calculation of buoyant mass.

$$\Delta P_f = (1-\varepsilon_f)(\rho_s - \rho_l)h_f = M_b g / A_c \quad [22]$$

For the prediction of the packed bed pressure drop Ergun's equation has been used.

$$\Delta P_{pa} = 150\frac{(1-\varepsilon_{pa})^2}{(\varepsilon_{pa})^3}\frac{\mu_l U_l h_{pa}}{(\varphi_s d_p)^2} + 1.75\frac{1-\varepsilon_{pa}}{(\varepsilon_{pa})^3}\frac{\rho_l U_l^2 h_{pa}}{\varphi_s d_p} \quad [23]$$

The pressure drop across the top grid depends on its design. With the column being empty the pressure drop across the top grid has been measured by increasing the liquid velocity. For the maximum liquid velocity of 0.3057 ms^{-1} used in the study the pressure drop across the bed has been found to be 400 Pa where as at the same liquid velocity the pressure drop in case of a semi-fluidized bed has been measured to be 52032 Pa for 0.00405 m particles with bed expansion ratio of 2.5. Thus the pressure drop across the top grid can be neglected in comparison to the semi-fluidized bed pressure drop. The semi-fluidized bed pressure drops have been calculated from the following equation.

$$\Delta P_{sf} = \frac{M_b g}{A_c} + 150\frac{(1-\varepsilon_{pa})^2}{(\varepsilon_{pa})^3}\frac{\mu_l U_l h_{pa}}{(\varphi_s d_p)^2} + 1.75\frac{1-\varepsilon_{pa}}{(\varepsilon_{pa})^3}\frac{\rho_l U_l^2 h_{pa}}{\varphi_s d_p} \quad [24]$$

In predicting the semi-fluidized bed pressure drop from Eq. (24), the packed bed voidage (ε_{pa}) has been assumed to be equal to the voidage of the reproducible initial static bed (ε_s). Fig. 18 shows the comparison of the experimentally measured semi-fluidized bed pressure drop with the values calculated from Eq. (24). Fairly good agreement between the values is obtained as most of the values are within 10%, but almost all the values predicted from Eq. (24) have been found to be lower than the experimental ones. The higher experimental pressure drop is expected for the packed bed as its actual voidage is little lower than the voidage of the static bed which has been used in the model Eq. (24). The top packed bed may be more compact than the initial static bed. The same phenomenon is prominent for small and irregular particles as reported by many earlier investigators. The compaction is not prominent in the present investigation

as the particles are regular in shape and larger in size and hence the deviations have been within -10%.

4. Conclusions

The present study of the liquid-solid semi-fluidized bed hydrodynamics has resulted in the following conclusions. Both the minimum and the maximum semi-fluidization velocities increase with the increase in particle size and bed expansion ratio, but decrease with the increase in liquid viscosity. The minimum semi-fluidization velocity is independent of the variation of initial static bed height, but the maximum semi-fluidization velocity increases with increase in the static bed height. Proposed Eqs. (2) and (5) in dimensional form and Eqs. (9) to (12) in dimensionless form can be suitably used for the prediction of the minimum and the maximum semi-fluidization velocities by selecting the proper one. Proposed Eqs. (17) through (20) can be used for the prediction of packed bed height in the semi-fluidized system with a caution that the Eq. (19) introduces a bit of uncertainty. Eq. (24) can suitably be used for the prediction of semi-fluidized bed pressure drop. The above correlations will be useful in the design of liquid-solid semi-fluidized bed systems for various process applications.

Nomenclature

A_c	cross-sectional area of bed, m^2
Ar	Archimedes number ($[d_p^3 \rho_l(\rho_s - \rho_l)g]/ \mu_l^2$), dimensionless
D_c	column (bed) diameter, m
d_p	mean particle diameter, m
g	acceleration of the gravity, m/s^2
h	height of the semi-fluidized bed, m
h_f	height of the expanded fluidized bed, m

h_{pa} height of the top packed bed, m

h_s height of the initial static bed, m

h_t height of the top restraining plate, m

M_b buoyant mass of the solid in the bed, kg

ΔP_f pressure drop across the fluidized section, Pa

ΔP_r pressure drop across the top restraining plate, Pa

ΔP_{pa} pressure drop across the packed section of the semi-fluidized bed, Pa

ΔP_{sf} pressure drop across the semi-fluidized bed, Pa

R bed expansion ratio, dimensionless

Re_t Reynolds number at terminal condition.

U_l superficial liquid velocity, m/s

U_{mf} minimum fluidization velocity, m/s

U_{msf} maximum semi-fluidization velocity, m/s

U_{osf} minimum semi-fluidization velocity, m/s

U_s semi-fluidization velocity, m/s

U_t particle terminal velocity, m/s

Greek symbols

ε_f porosity of fluidized bed, dimensionless

ε_{pa} porosity of packed section, dimensionless

ε_s porosity of reproducible static bed

μ_l liquid viscosity, Pa s

μ_w viscosity of water, Pa s

φ_s sphericity of solid particle, dimensionless

ρ_l density of liquid, kg/m^3

ρ_s density of solid, kg/m^3

References

[1] J. S. N. Murthy, G. K. Roy, Semi-fluidization: a Review, Indian chem. Eng. 29 (2) (1986) 9-22.

[2] T. C. Ho, S. J. Yau, J. R. Hopper, Hydrodynamics of Semi-fluidization in gas-solid systems, Powder Technol. 50 (1987) 25-34.

[3] S. M. M. Dias, Extractive fermentation of ethanol by immobilized yeast cells, Report, Dep. Eng., Tech. Univ. Lisbon, Lisbon, Port., 218 pages, 1991.

[4] R. L. Is'emin, N. A. Zaitseva, A. D. Osipov, A. P. Akol'zin, Formation of nitrogen oxides and deposits on the heating surfaces of boilers with semi-fluidized bed furnaces fired with low grade coal, Promyshlennaya Energetika. 2 (1995) 37-38.

[5] S. J. Hwang, W. J. Lu, Ion Exchange in a Semi-fluidized Bed, Ind. Eng. Chem. Res. 34 (1995)1434-1439.

[6] S. J. Kim, S. Y. Jeung, H. Moon, Removal and recovery of heavy metal ions in fixed and semi-fluidized beds, Korean J. Chem. Eng. 15 (1998) 637-643.

[7] J.Y. Hristov, Magnetic semifluidization of gas-fluidized ferromagnetic particles, Hung. J. Ind. Chem. 26(1998) 69-75.

[8] S. J. Kim, K. R. Hwang, S. Y. Cho, Study on ion-exchange behavior of Cu-CN complexes, J. Chem. Eng. Jpn. 34 (2001) 193-198.

[9] R. L. Is'emin, V. V. Konyakhin, S. N. Kuz'min, E. V. Budkova, Boiler for central heating operating on low-grade solid fuel, Promyshlennaya Energetika. 9 (2001) 22-25.

[10] T. C. Ho, N. Kobayashi, Y. K. Lee, C. J. Lin, J. R. Hopper, Modeling of mercury sorption by activated carbon in a confined, a semi-fluidized, and a fluidized bed, Waste Manage. 22 (2002) 391-398.

[11] T. C. Ho, Y. K. Lee, J. R. Hopper, C. J. Lin, N. Kobayashi, Mercury emission control from combustion flue gas employing semi-fluidized bed activated carbon adsorption, J. Chin. Inst. Chem. Eng. 36 (2005) 77-84.

[12] T. Y. Kim, J. Kim, S. Y. Cho, Separation characteristics of phenoxyacetic acids in fixed and semi - fluidized beds, Stud. Surf. Sci. Cat. 159 (2006) 513-516.

[13] X. Liu, G. Xu, S. Gao, Fluidization of extremely large and widely sized coal particles as well as its application in an advanced chain grate boiler, Powder Technol. 188 (2008) 23-29.

[14] S. Dehkissia, A. Baçaoui, I. Iliuta, F. Larachi, Dynamics of fines deposition in an alternating semifluidized bed, AIChE J. 54 (2008) 2120-2131.

[15] C. Liu, Z. Li, W. Zheng, X. Wen, H. Liu, Method for manufacturing charging coal from blend coal for coking, Anshan Coking and Refractory Engineering Consulting Corporation, China Metallurgical Construction Group, Peop. Rep. China, 2006, CNXXEV CN 1834204 A 20060920 Patent written in Chinese. Application: CN 1003-1537 20060421.

[16] J. Kurian, M. Raja Rao, Hydrodynamics of semi-fluidized bed, Indian J. Tech. 8 (1970) 275-284.

[17] L.T. Fan, E.H. Hsu, "Semifluidized Bed Bioreactor," in *Advances in Biotechnology* (Proceedings of the VIth International Fermentation Symposium, London, Ontario,

Canada, July 20-25, 1980), Vol. I, ed. by M. Moo-Young, pp. 663-669, Pergamon Press, New York, N.Y. 1981.

[18] L. T. Fan, C. Y. Wen, Mechanics of semi-fluidization of single size particles in solid-liquid systems, AIChE J. 7 (1961) 606-610.

[19] G. K. Roy, K. J. R. Sarma, Dynamics of liquid-solid semi-fluidization III: Relation between onset of semi-fluidization and minimum fluidization velocity, Chem. Eng. J. 4 (1972) 294-296.

[20] G. K. Roy, H. N. Sharat Chandra, Liquid-solid semi-fluidization of heterogeneous mixtures II: Prediction of minimum semi-fluidization velocity, Chem. Eng. J. 12 (1976) 77-80.

[21] C. K. Gupta and D. Sathiyamoorthy, Fluid bed technology in material processing, CRC Press, Florida, 1999, 38.

[22] G. K. Roy, Studies on certain aspects of semi-fluidization, PhD Thesis, Sambalpur University, India, 1975.

[23] C. Y. Wen, Y. H. Yu, A generalized method for predicting the minimum fluidization velocity, AIChE J. 12 (1966) 610-612.

[24] G. K. Roy, K. J. R. Sarma, Relation between maximum semi-fluidization and minimum fluidization velocity in liquid-solid systems, J. Inst. Eng. (India) 54-CH2 (1974) 34-35.

[25] A. N. Singh, H. R. Takhalate, A. Storck, P. Sen Gupta, A correlation for the prediction of packed bed height in liquid-solid semi-fluidization, Chem. Eng. J. 20 (1980) 69-73.

[26] J. Mydlarz, Prediction of the packed bed height in liquid-solid semi-fluidization of homogeneous mixtures, Chem. Eng. J. 34 (1987) 155-158.

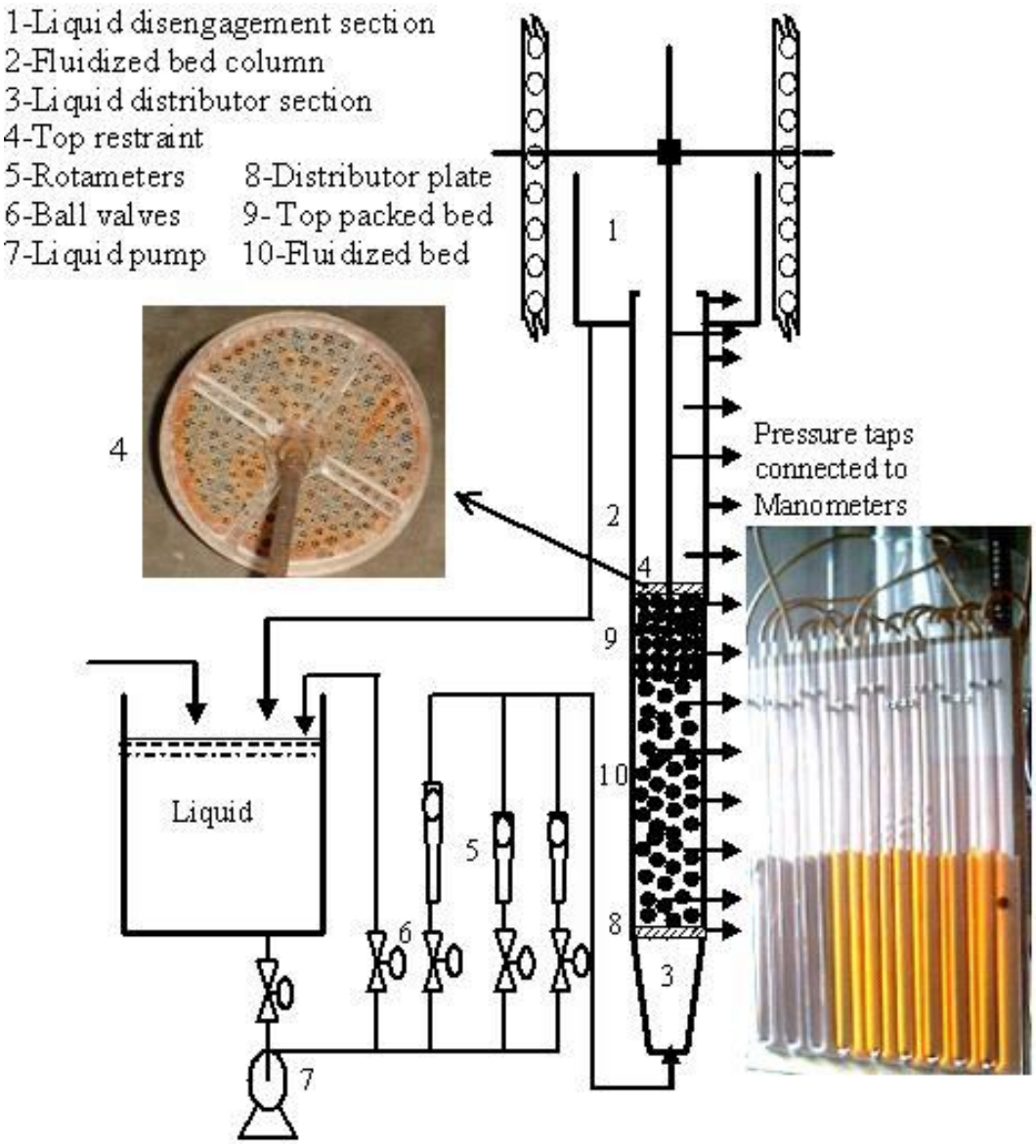

Fig. 1. Experimental setup.

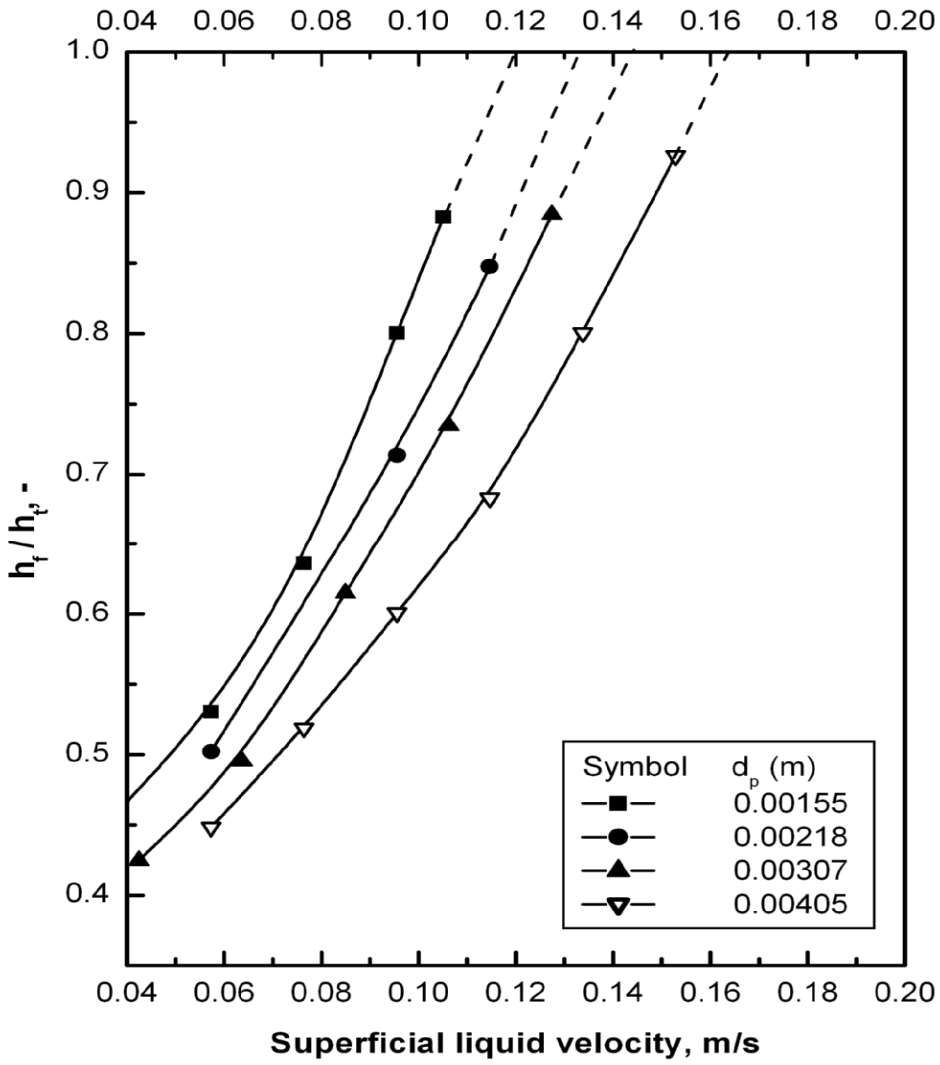

Fig. 2. Variation of h_f/h_t with U_l for glass beads and water with h_s=0.171 m and R=2.5.

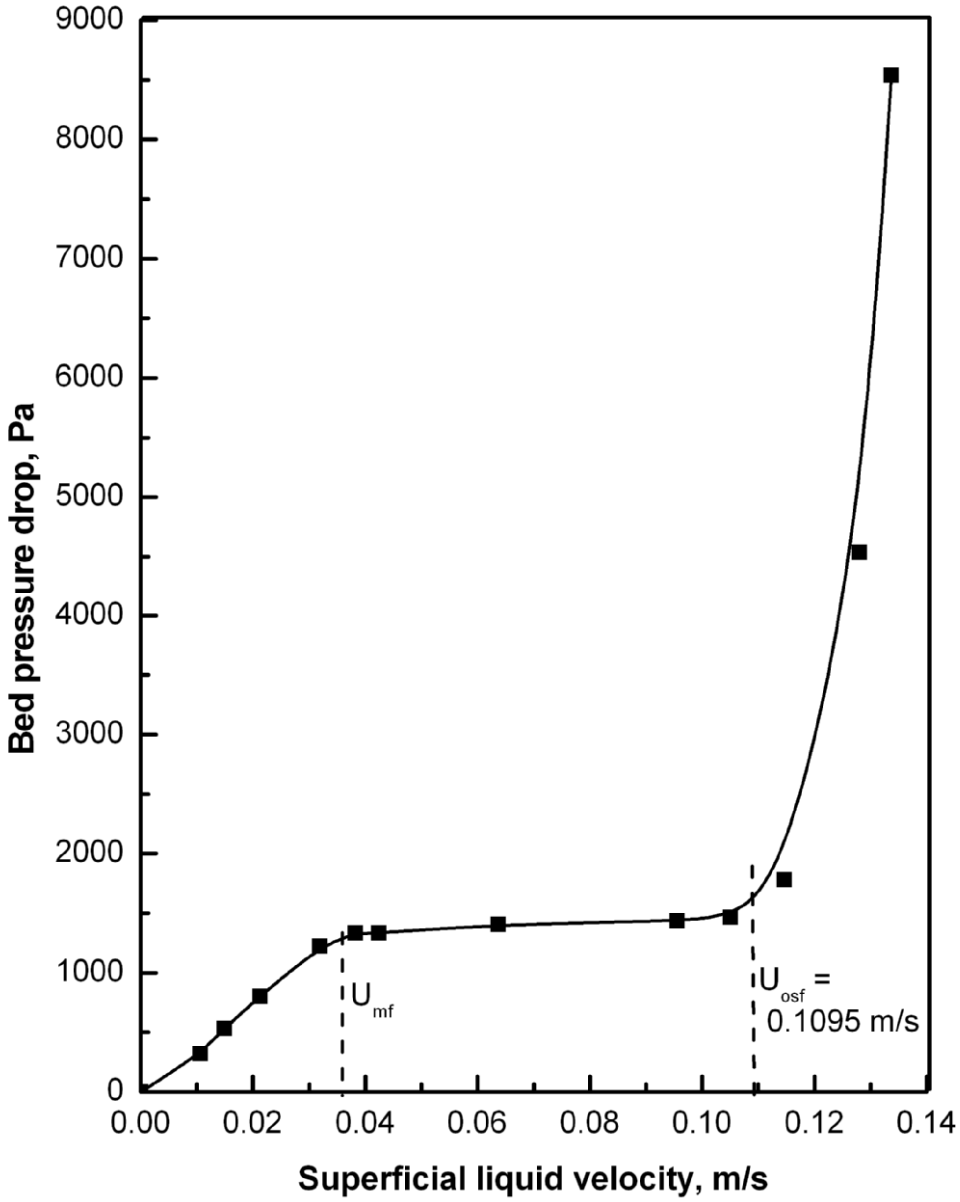

Fig. 3. Variation of bed pressure drop with U_l for 0.00218 m particles in water with h_s=0.171 m and R=2.5.

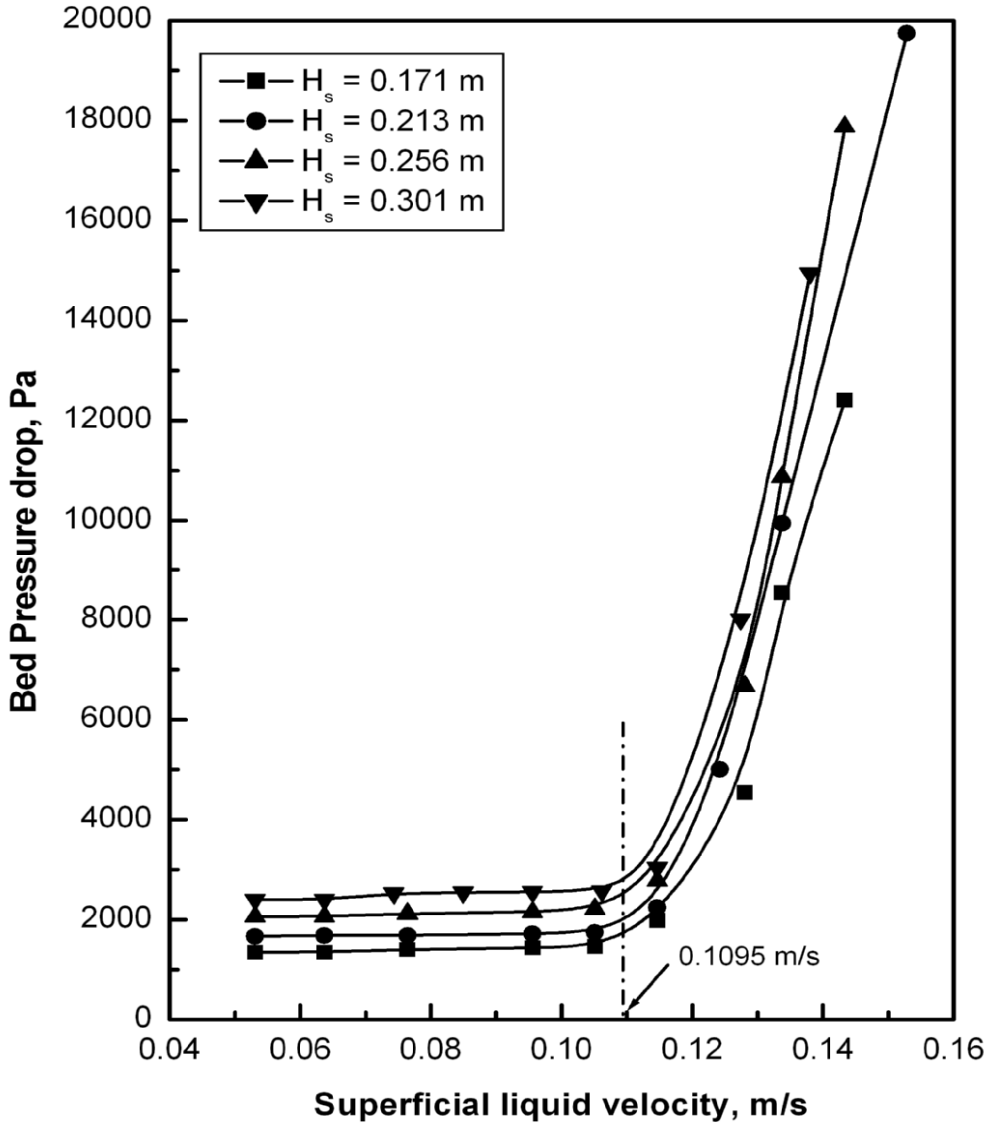

Fig. 4. Variation of bed pressure drop with U_l for 0.00218 m particles in water at different h_s with R=2.5.

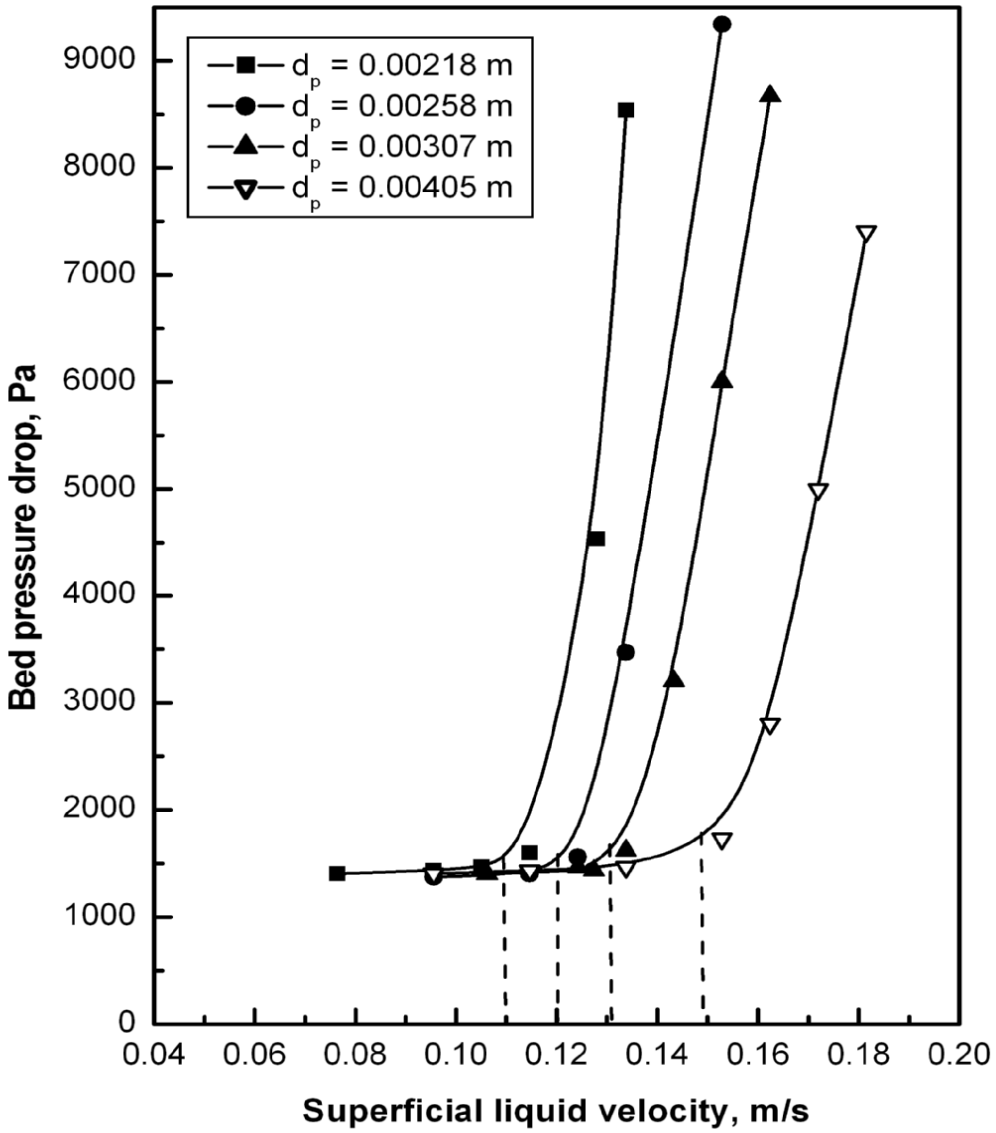

Fig. 5. Variation of bed pressure drop with U_l for different particle sizes in water with h_s=0.171 m and R=2.5.

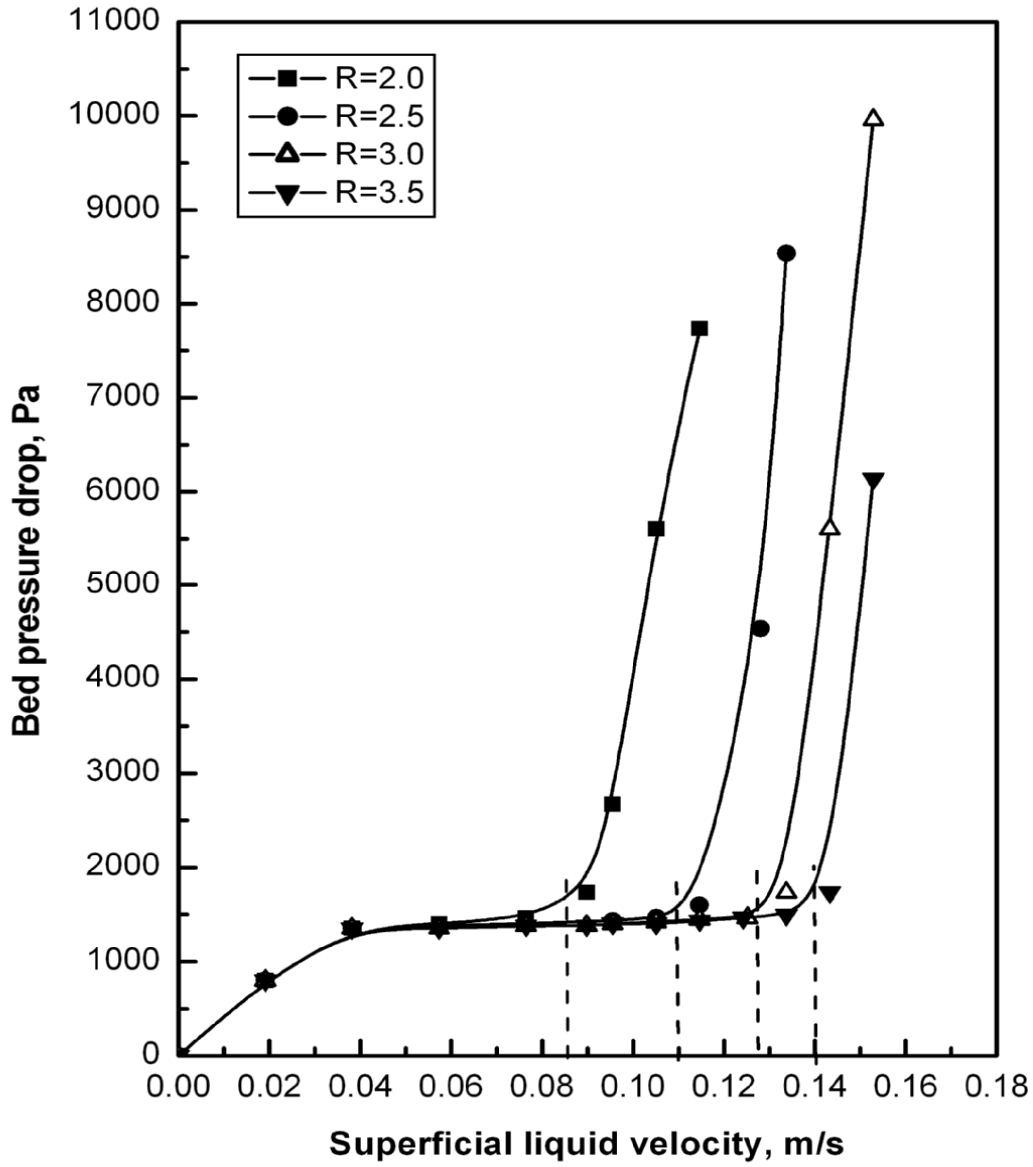

Fig. 6. Variation of bed pressure drop with U_l for 0.00218 m particles in water at different R with h_s=0.171 m.

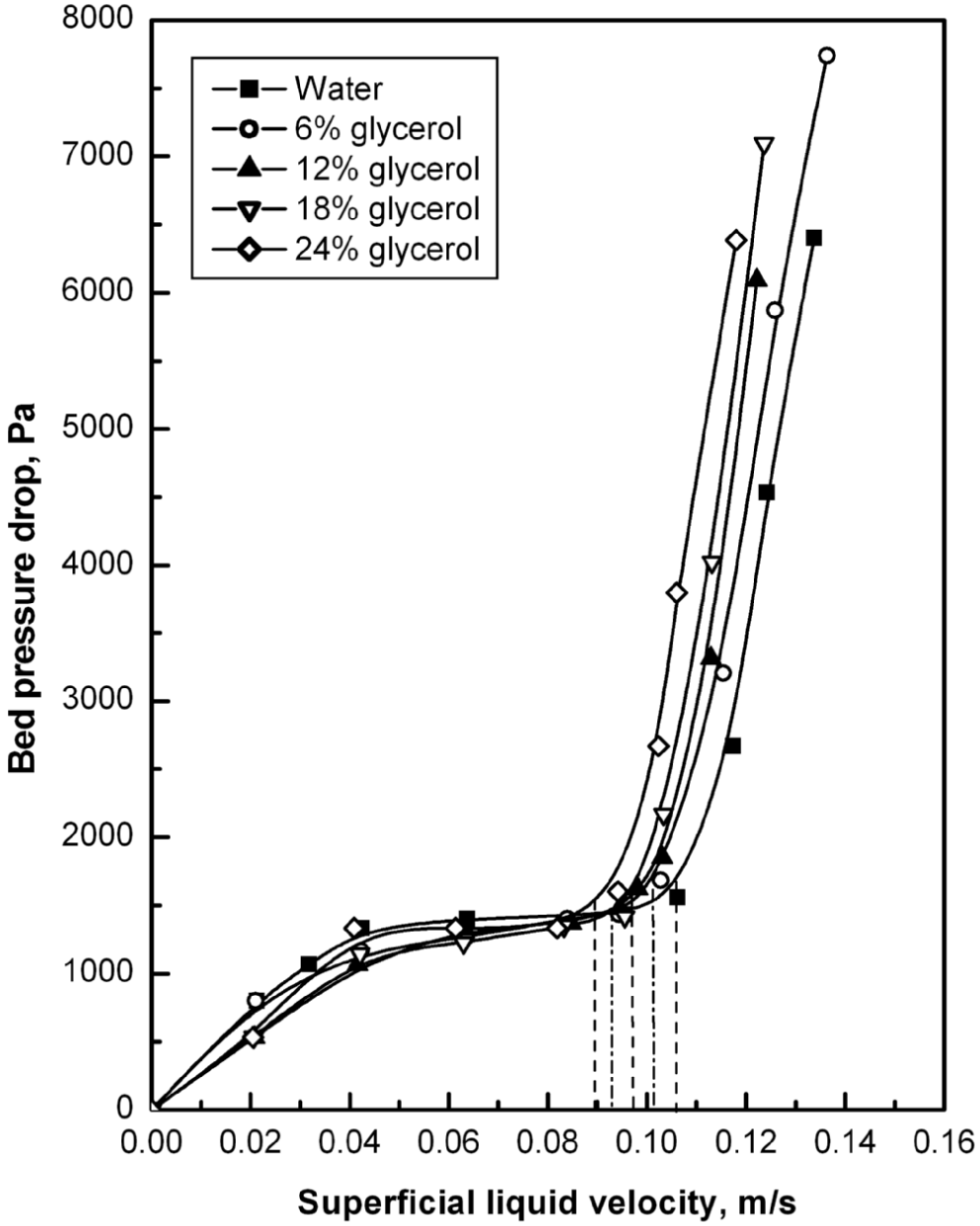

Fig. 7. Variation of bed pressure drop with U_l for 0.00307 m particles in aqueous solution of glycerol of different composition at h_s=0.171 m and R=2.0.

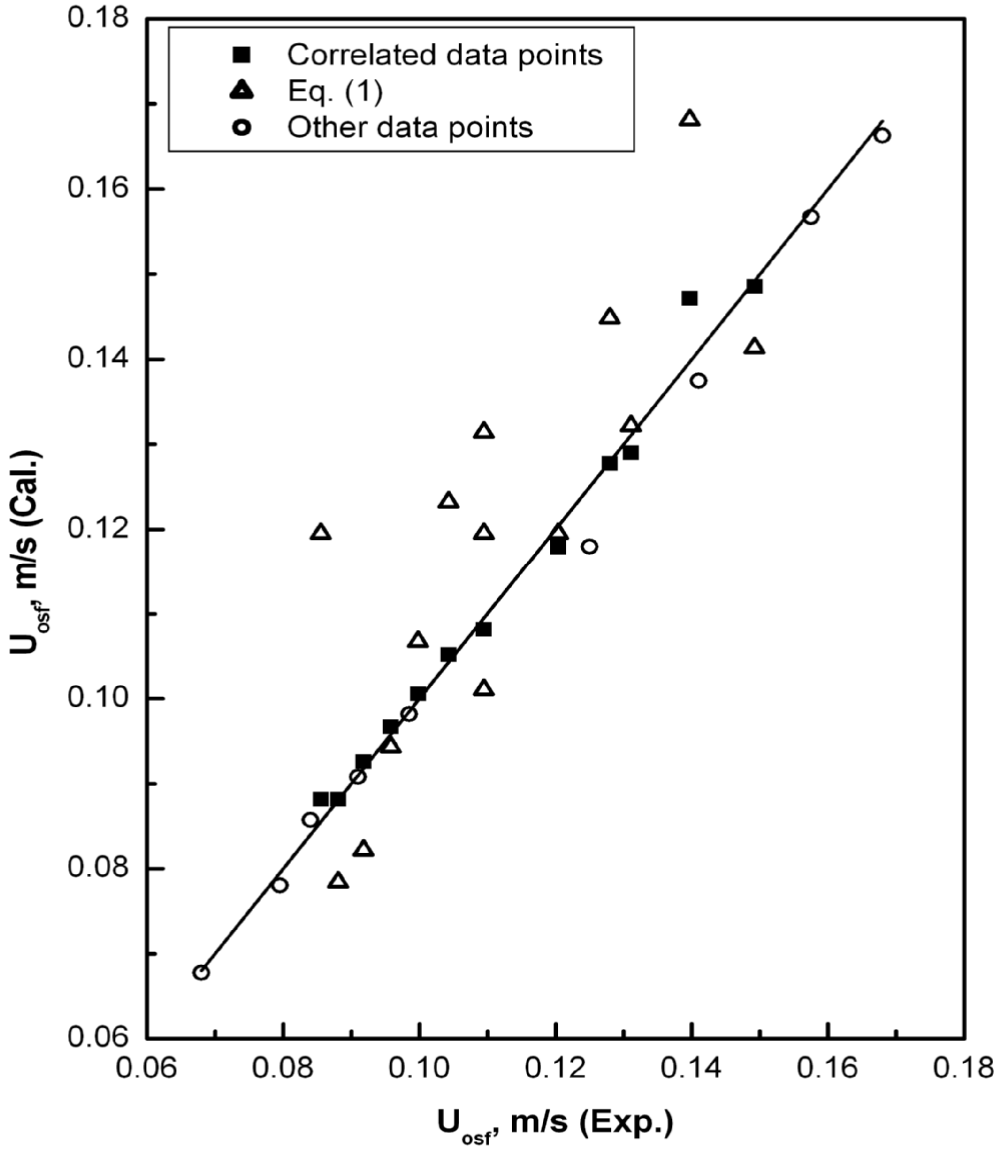

Fig. 8. Comparison of minimum semi-fluidization velocities.

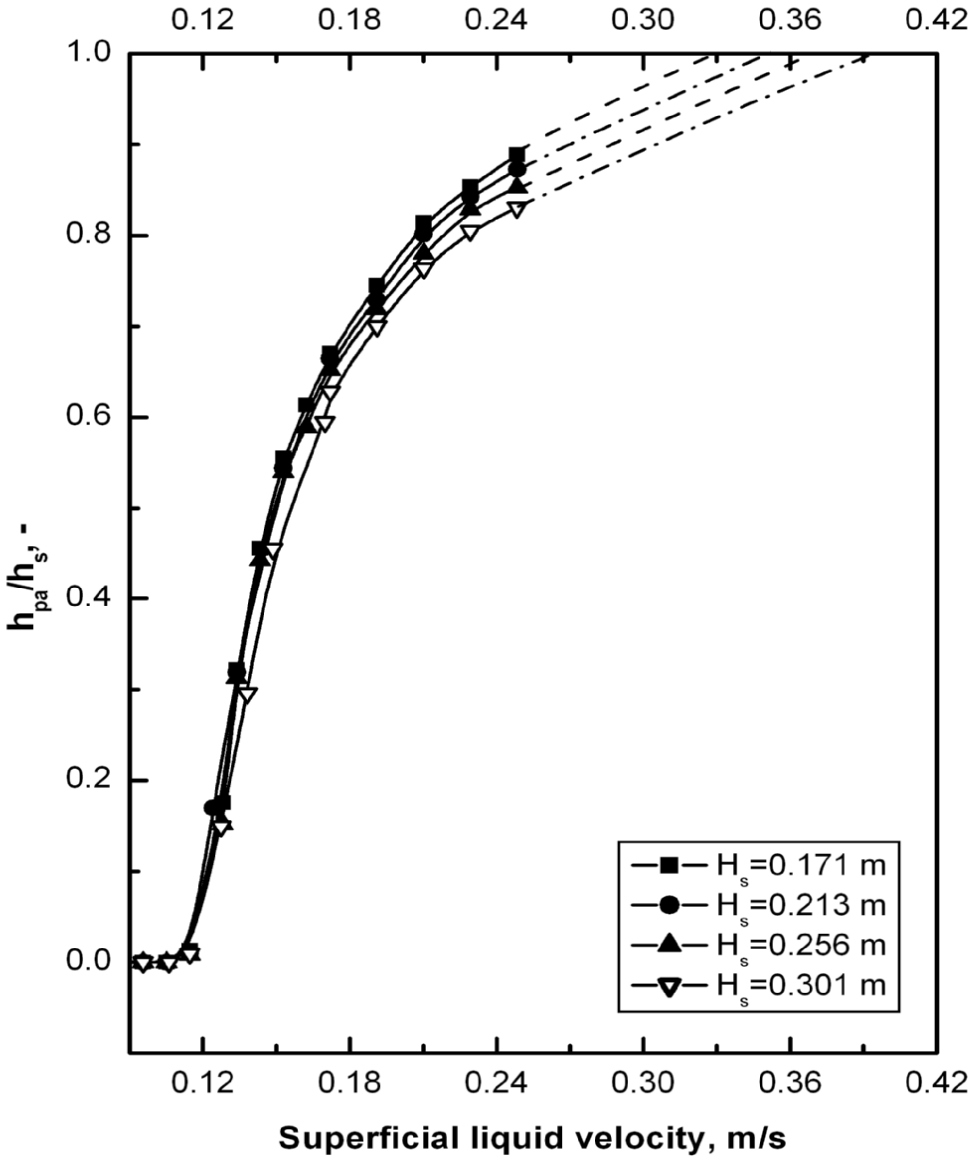

Fig. 9. Variation of h_{pa}/h_s with U_l for 0.00218 m particles in water at different h_s with R=2.5.

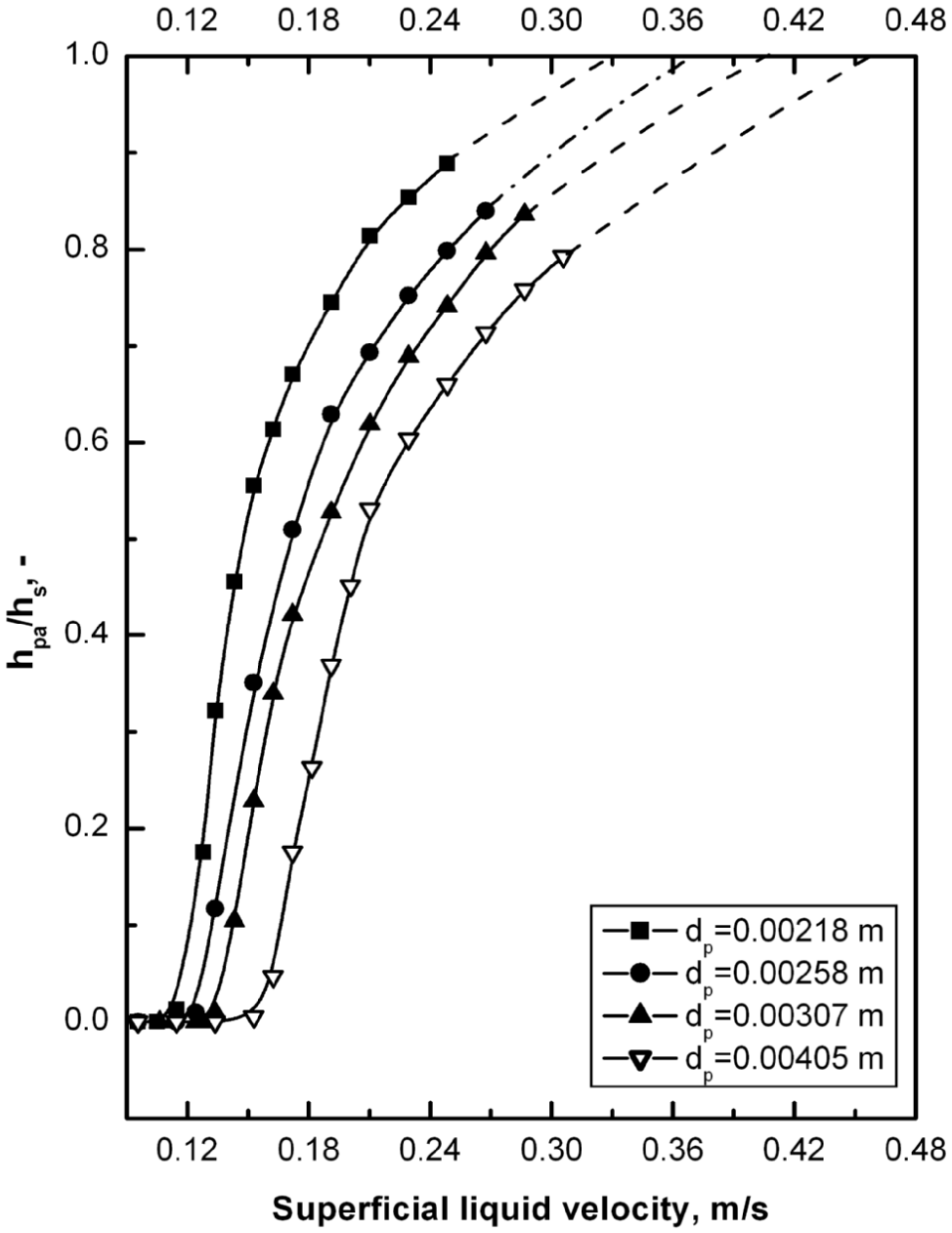

Fig. 10. Variation of h_{pa}/h_s with U_l for different particle sizes in water with h_s=0.171 m and R=2.5.

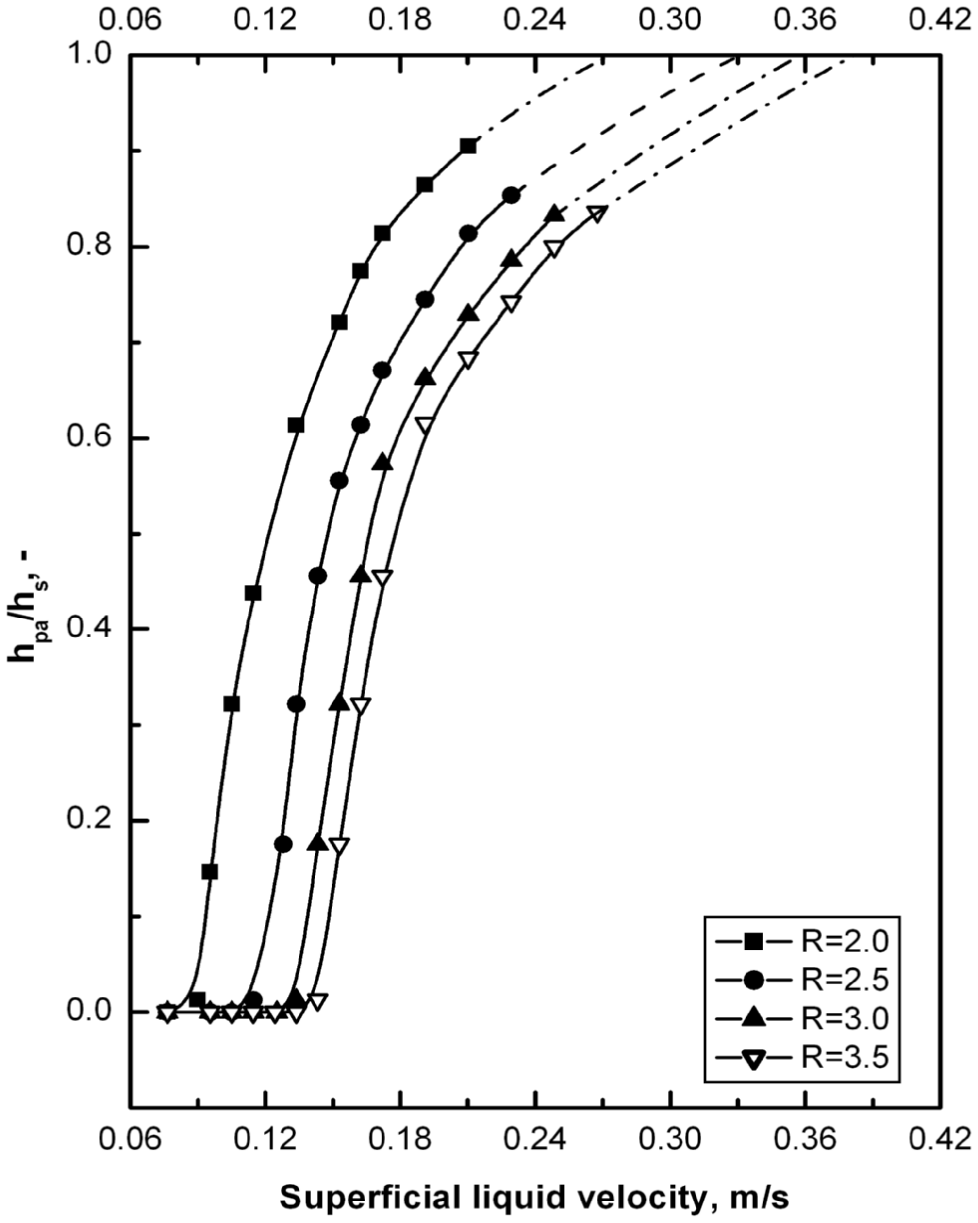

Fig. 11. Variation of h_{pa}/h_s with U_l for 0.00218 m particles in water at different R with h_s=0.171 m.

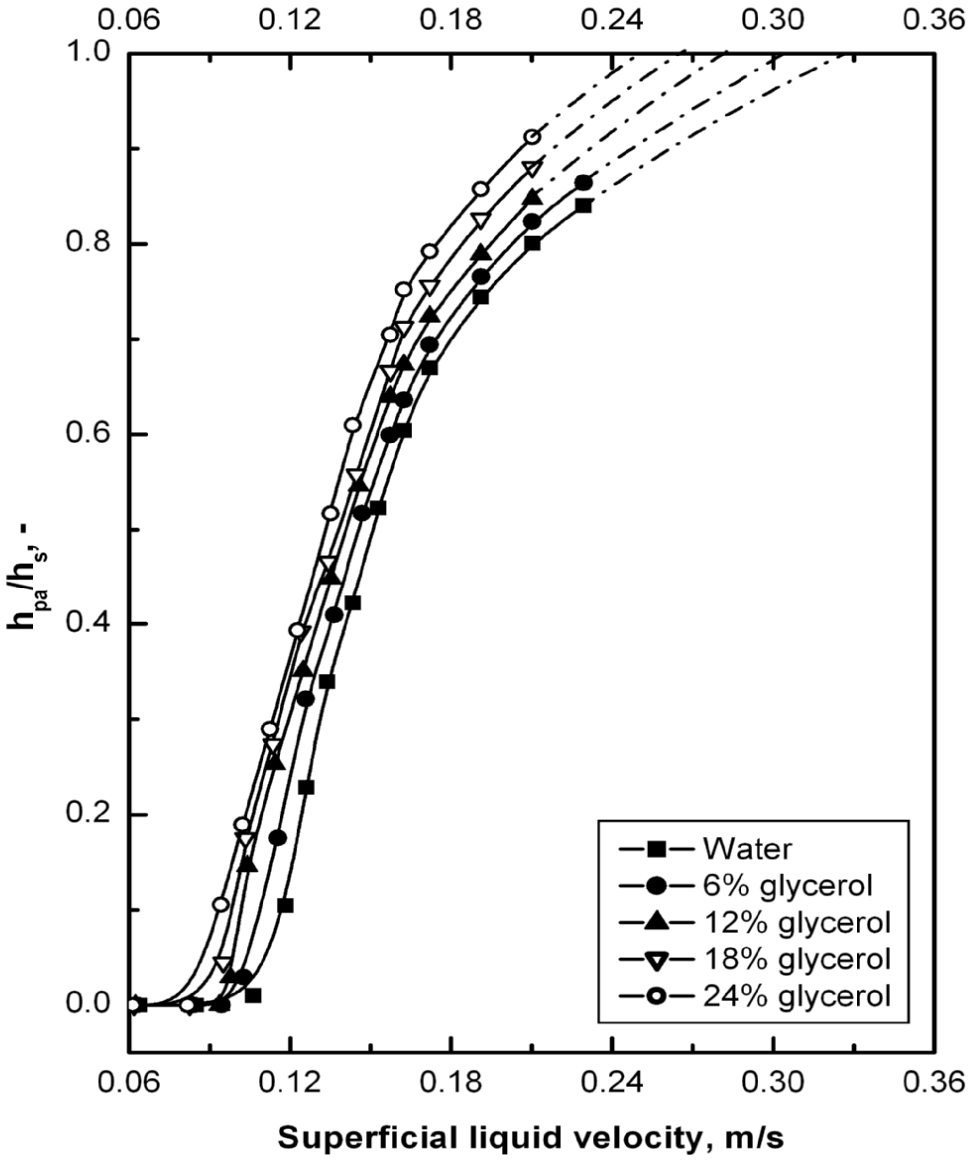

Fig. 12. Variation of h_{pa}/h_s with U_l for 0.00307 m particles in aqueous solution of glycerol of different composition at h_s=0.171 m and R=2.0.

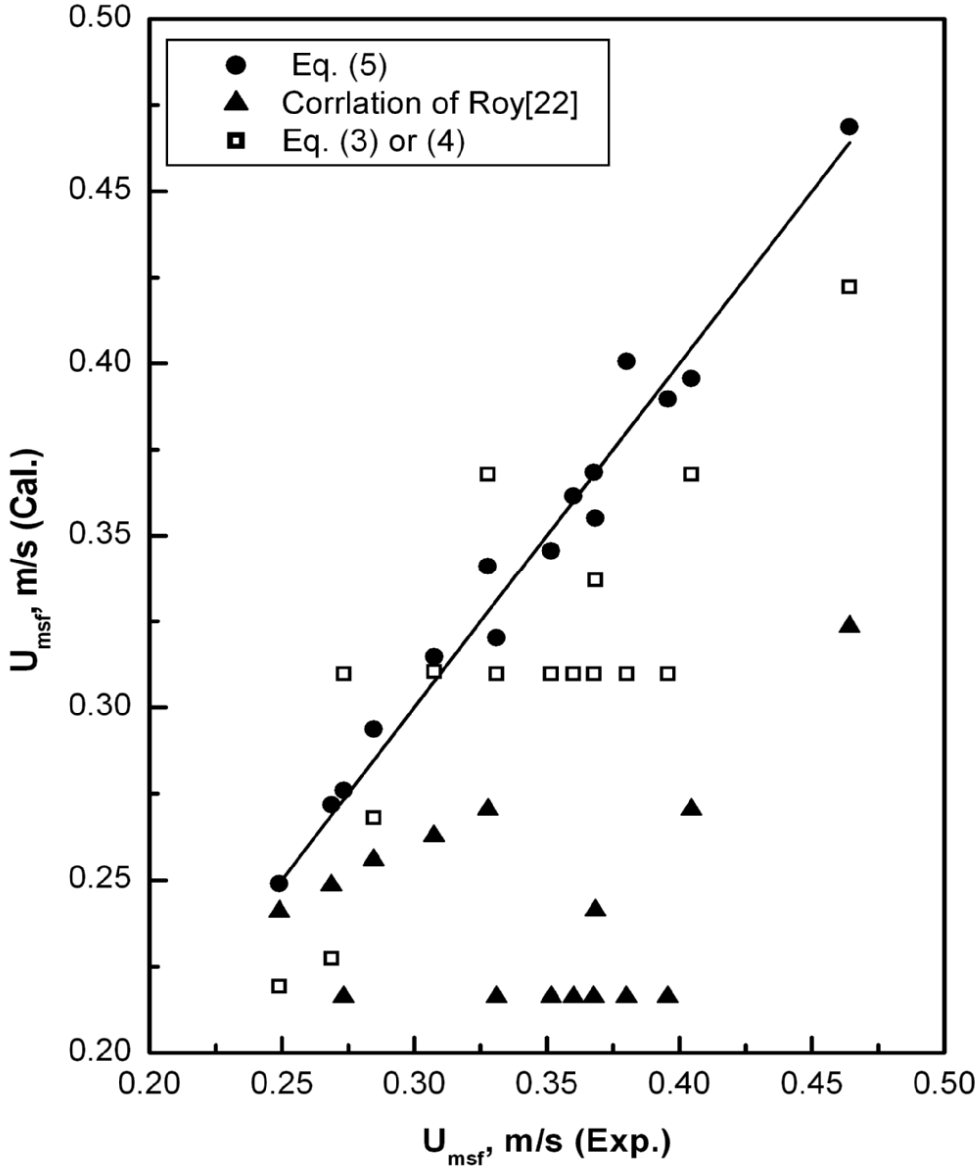

Fig. 13. Comparison of maximum semi-fluidization velocities.

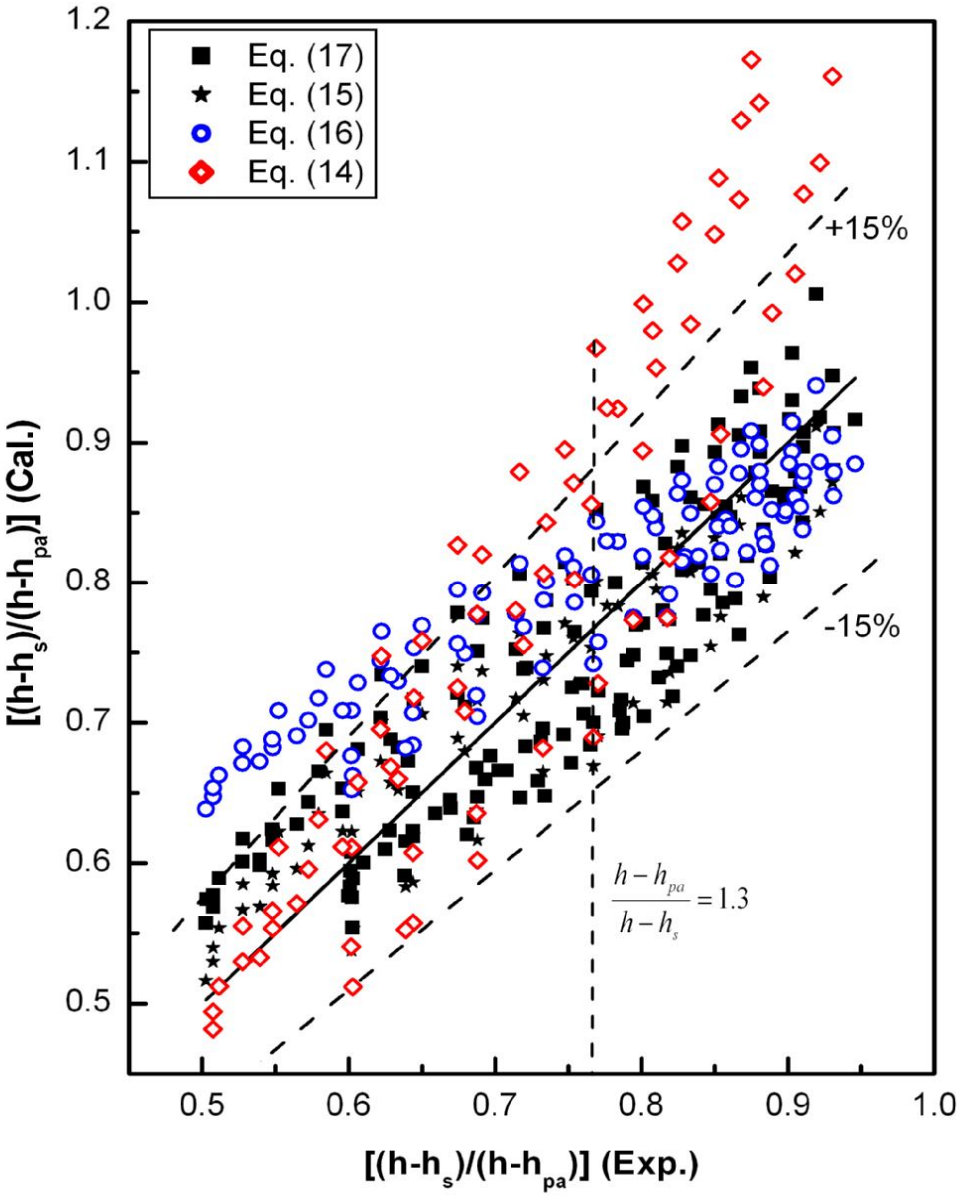

Fig. 14. Comparison of dimensionless packed bed height ($(h\text{-}h_s)/h\text{-}h_{pa}$).

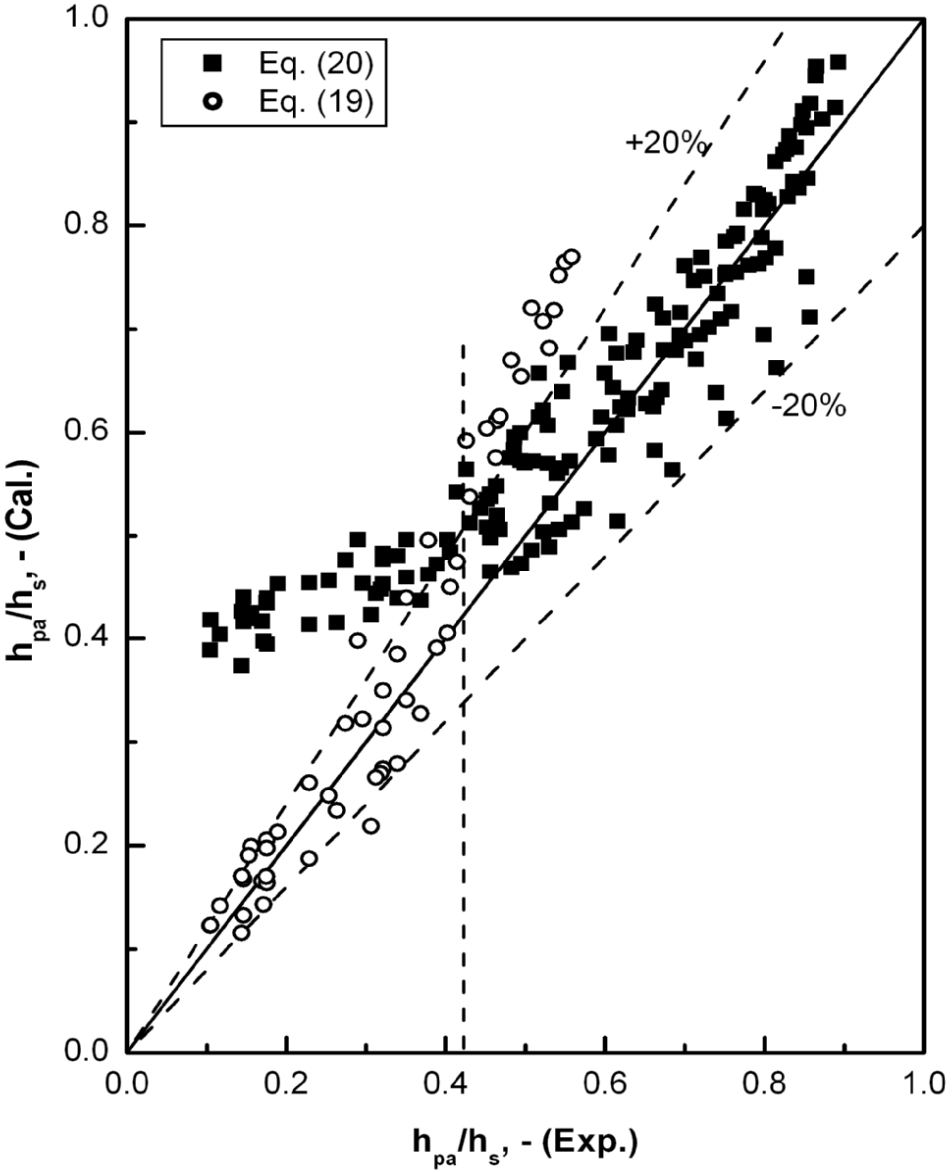

Fig. 15. Comparison of dimensionless packed bed height (h_{pa}/h_s).

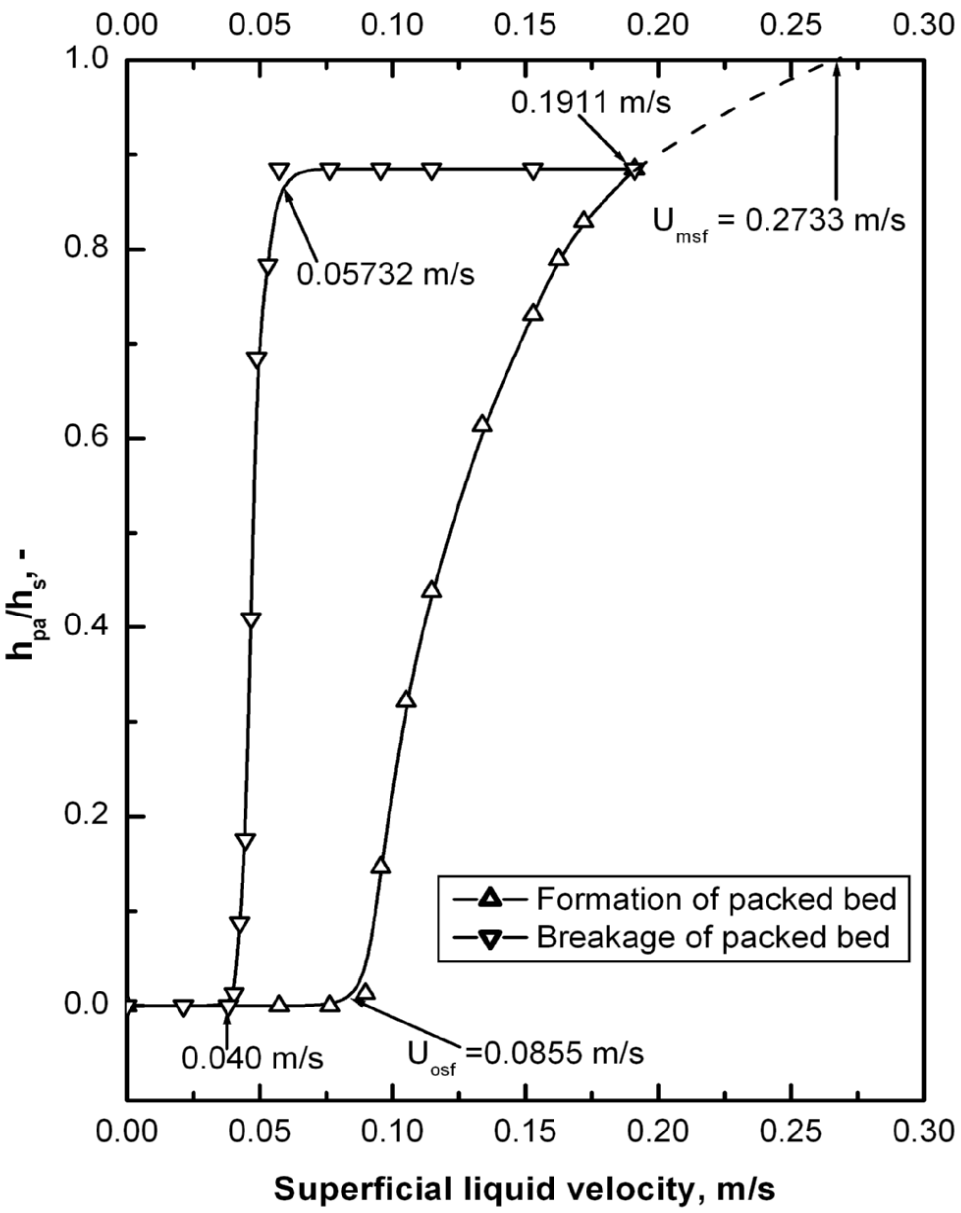

Fig. 16. Formation and breakage of packed bed with variation of liquid velocity for 0.00218 m particles at h_s=0.171 m and R=2.0.

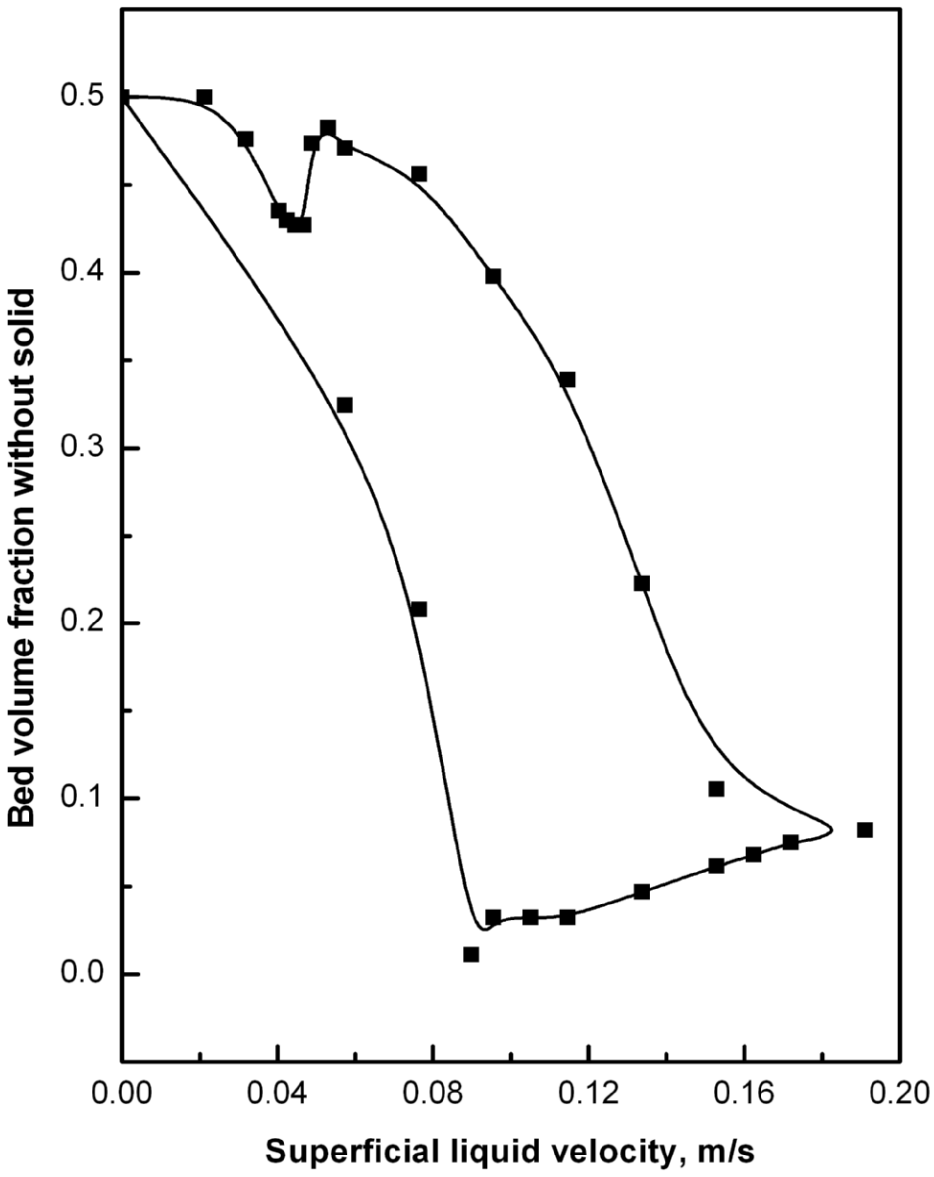

Fig. 17. Variation of Bed volume fraction without solids with liquid velocity for 0.00218 m particles at h_s=0.171 m and R=2.0.

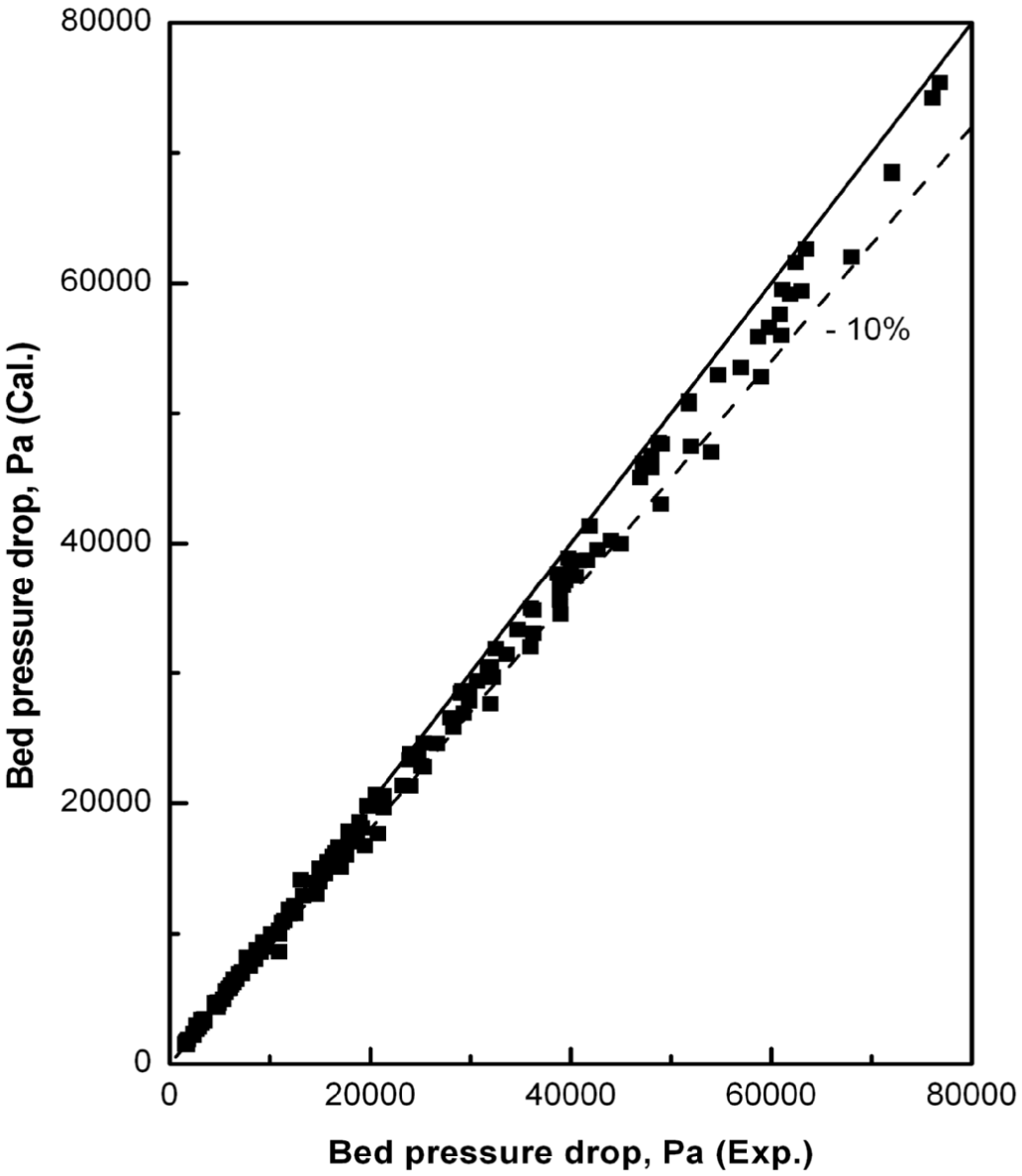

Fig. 18. Comparison of semi-fluidized bed pressure drop.

Table 1

Characteristics of particle-liquid system used in the study.

Solid-liquid system	d_p, mm	ρ_p, kg/m^3	ε_s, -	ρ_l, kg/m^3	μ_lx10^3, Pa.s	h_s, m	R, -
Glass beads-water	2.18	2470	0.425	995.7	0.789	0.171	2.5
do	2.18	2470	0.425	995.7	0.789	0.213	2.5
do	2.18	2470	0.425	995.7	0.789	0.256	2.5
do	2.18	2470	0.425	995.7	0.789	0.301	2.5
do	2.58	2470	0.423	995.7	0.789	0.171	2.5
do	3.07	2470	0.420	995.7	0.789	0.171	2.5
do	4.05	2470	0.415	995.7	0.789	0.171	2.5
do	2.18	2470	0.425	995.7	0.789	0.171	2.0
do	2.18	2470	0.425	995.7	0.789	0.171	3.0
do	2.18	2470	0.425	995.7	0.789	0.171	3.5
do	3.07	2470	0.420	995.7	0.789	0.171	2.0
Glass beads- aqueous solution of glycerol. % by mass of glycerol							
6.0	3.07	2470	0.420	1009.7	0.948	0.171	2.0
12.0	3.07	2470	0.420	1024.0	1.082	0.171	2.0
18.0	3.07	2470	0.420	1039.0	1.268	0.171	2.0
24.0	3.07	2470	0.420	1054.0	1.567	0.171	2.0

Table 2

Minimum and maximum semi-fluidization velocities.

h_s (m)	d_p (mm)	R	μ_lx10^3 (Pa.s)	U_{mf}^{*} (m/s)	U_{osf}^{**1} (m/s)	U_{osf}^{**2} (m/s)	U_{osf}^{***} (m/s)	U_{msf}^{**} (m/s)	$U_t^{\$}$ (m/s)	$U_{msf}^{\#}$ (m/s)
0.171	2.18	2.5	0.798	0.0256	0.1214	0.1095	0.1195	0.3310	0.3098	0.2163
0.213	2.18	2.5	0.798	0.0256	0.1214	0.1095	0.1195	0.3516	0.3098	0.2163
0.256	2.18	2.5	0.798	0.0256	0.1214	0.1095	0.1195	0.3677	0.3098	0.2163
0.301	2.18	2.5	0.798	0.0256	0.1214	0.1095	0.1195	0.3956	0.3098	0.2163
0.171	2.58	2.5	0.798	0.0302	0.1326	0.1204	0.1315	0.3683	0.3370	0.2413
0.171	3.07	2.5	0.798	0.0348	0.1444	0.1311	0.1449	0.4045	0.3679	0.2705
0.171	4.05	2.5	0.798	0.0428	0.1639	0.1492	0.1682	0.4642	0.4222	0.3235
0.171	2.18	2.0	0.798	0.0256	0.9892	0.0855	0.1011	0.2733	0.3098	0.2163
0.171	2.18	3.0	0.798	0.0256	0.1385	0.1280	0.1322	0.3602	0.3098	0.2163
0.171	2.18	3.5	0.798	0.0256	0.1520	0.1397	0.1414	0.3801	0.3098	0.2163
0.171	3.07	2.0	0.798	0.0348	0.1180	0.1043	0.1232	0.3278	0.3679	0.2705
0.171	3.07	2.0	0.948	0.0331	0.1113	0.0998	0.1068	0.3074	0.3104	0.2628
0.171	3.07	2.0	1.082	0.0316	0.1065	0.0958	0.0943	0.2846	0.2680	0.2559
0.171	3.07	2.0	1.268	0.0297	0.1035	0.0918	0.0822	0.2687	0.2273	0.2486
0.171	3.07	2.0	1.567	0.0275	0.0983	0.0881	0.0784	0.2492	0.2193	0.2410

[*] Calculated from the correlation of Wen and Yu [23].
[**] Experimental values. [1] method-1, [2] method-2.
[***] Calculated from the correlation of Kurian and Raja Rao [16].
[$] Calculated from Intermediate law or Newton's law [21].
[#] Calculated from the correlation of Roy [22].

Table 3

Dimensionless minimum and maximum semi-fluidization velocities.

$\frac{h_s}{D_c}$	$\frac{d_p}{D_c}$	R	$\frac{\mu_l}{\mu_w}$	$\frac{U_{osf}}{U_{mf}}$ *	$\frac{U_{osf}}{U_{mf}}$ **	$\frac{U_{osf}}{U_{msf}}$ *	$\frac{U_{osf}}{U_{msf}}$ &	$\frac{U_{msf}}{U_{mf}}$ *	$\frac{U_{msf}}{U_{mf}}$ #
1.71	0.0218	2.5	1.000	4.272	7.208	0.3308	0.3638	12.91	15.49
2.13	0.0218	2.5	1.000	4.272	7.208	0.3114	0.3638	13.72	15.49
2.56	0.0218	2.5	1.000	4.272	7.208	0.2978	0.3638	14.35	15.49
3.01	0.0218	2.5	1.000	4.272	7.208	0.2768	0.3638	15.44	15.49
1.71	0.0258	2.5	1.000	4.013	6.892	0.3269	0.3763	12.28	14.43
1.71	0.0307	2.5	1.000	3.767	6.578	0.3241	0.3897	11.62	13.41
1.71	0.0405	2.5	1.000	3.486	6.113	0.3214	0.4118	10.85	11.94
1.71	0.0218	2.0	1.000	3.336	6.326	0.3128	0.3342	10.66	15.49
1.71	0.0218	3.0	1.000	4.994	8.019	0.3556	0.3899	11.62	13.41
1.71	0.0218	3.5	1.000	5.451	8.776	0.3676	0.4134	10.85	11.94
1.71	0.0307	2.0	1.000	2.997	5.773	0.3182	0.3580	9.419	13.41
1.71	0.0307	2.0	1.188	3.011	5.791	0.3247	0.3572	9.276	13.53
1.71	0.0307	2.0	1.378	3.036	5.809	0.3366	0.3563	9.091	13.66
1.71	0.0307	2.0	1.629	3.092	5.829	0.3416	0.3554	9.050	13.79
1.71	0.0307	2.0	1.967	3.204	5.848	0.3538	0.3546	9.024	13.93

* Experimental values.
** Calculated from the correlation of Roy and Sarma [19].
& Calculated from the correlation of Roy and Sharat Chandra [20].
# Calculated from the correlation of Roy and Sarma [24].